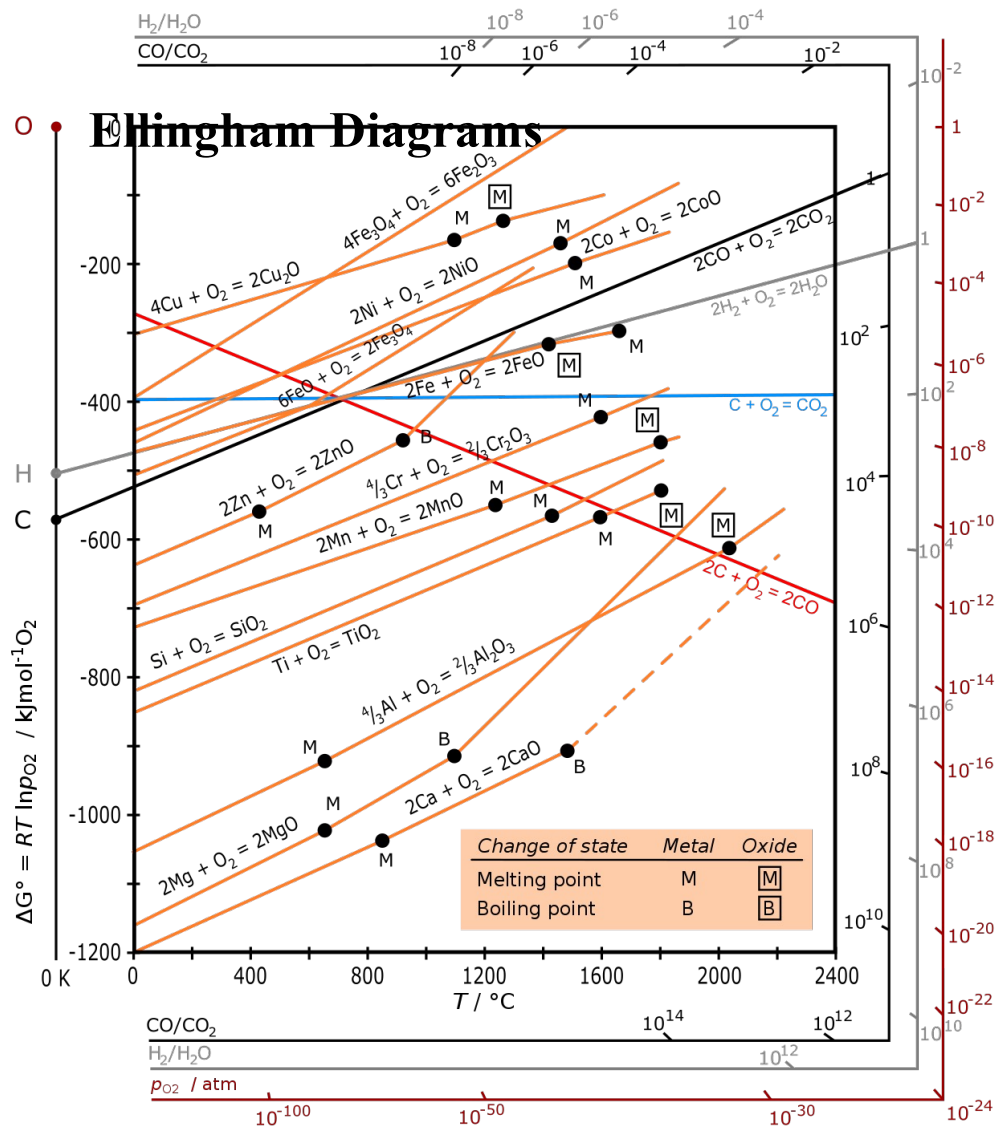


Dependencies of the Heat of Formation

Reference State: Elemental ground state at STP has an enthalpy of formation of 0 N_2 , O_2 , He etc.

		$\Delta H_{f,298.15}$	$\Delta G_{f,298.15}$	Heat Capacity Constants			
		kJ/mol	kJ/mol	A	B	C	D
Solids: Standard state is pure solid at 298.15 K, 1 bar.							
	Carbon (graphite) (298-1300 K)	0	0	-3.958	5.586E-02	-4.548E-05	1.517E-08
	Calcium carbonate, CaCO ₃	-1206.92	-1128.79				
	Calcium oxide, CaO	-635.09	-604.03				
	Glucose	-1273.3	-908.1				
Miscellaneous Gases							
899	Nitrous oxide	82.05	103.638	21.62	0.07281	-5.778E-05	1.830E-08
901	Oxygen	0	0	28.11	-3.7E-06	1.746E-05	-1.065E-08
902	Hydrogen (equilibrium)	0	0	27.14	0.009274	-1.381E-05	7.645E-09
905	Nitrogen	0	0	31.15	-0.01357	2.680E-05	-1.168E-08
908	Carbon monoxide	-110.53	-137.16	30.87	-0.01285	2.789E-05	-1.272E-08
910	Sulfur dioxide	-296.81	-300.14	23.85	0.06699	-4.961E-05	1.328E-08
911	Sulfur trioxide	-396.0	-371.3	19.21	0.1374	-1.176E-04	3.700E-08
912	Nitric oxide	90.25	86.58	29.35	-0.00094	9.747E-06	-4.187E-09
913	Helium-4	0	0	20.8			
914	Argon	0	0	20.8			
917	Fluorine	0	0				
918	Chlorine	0	0	26.93	0.03384	-3.869E-05	1.547E-08
919	Neon	0	0	20.8			
920	Krypton	0	0	20.8			
922	Bromine	0	0	33.86	0.01125	-1.192E-05	4.534E-09
959	Xenon	0	0	20.8			

Generally, energy is released on formation of a molecule from the elements if the molecule is stable, so the heat of formation is generally negative. For unstable molecules such as NO which is a radical formed at high temperatures, the heat of formation is positive (endothermic).



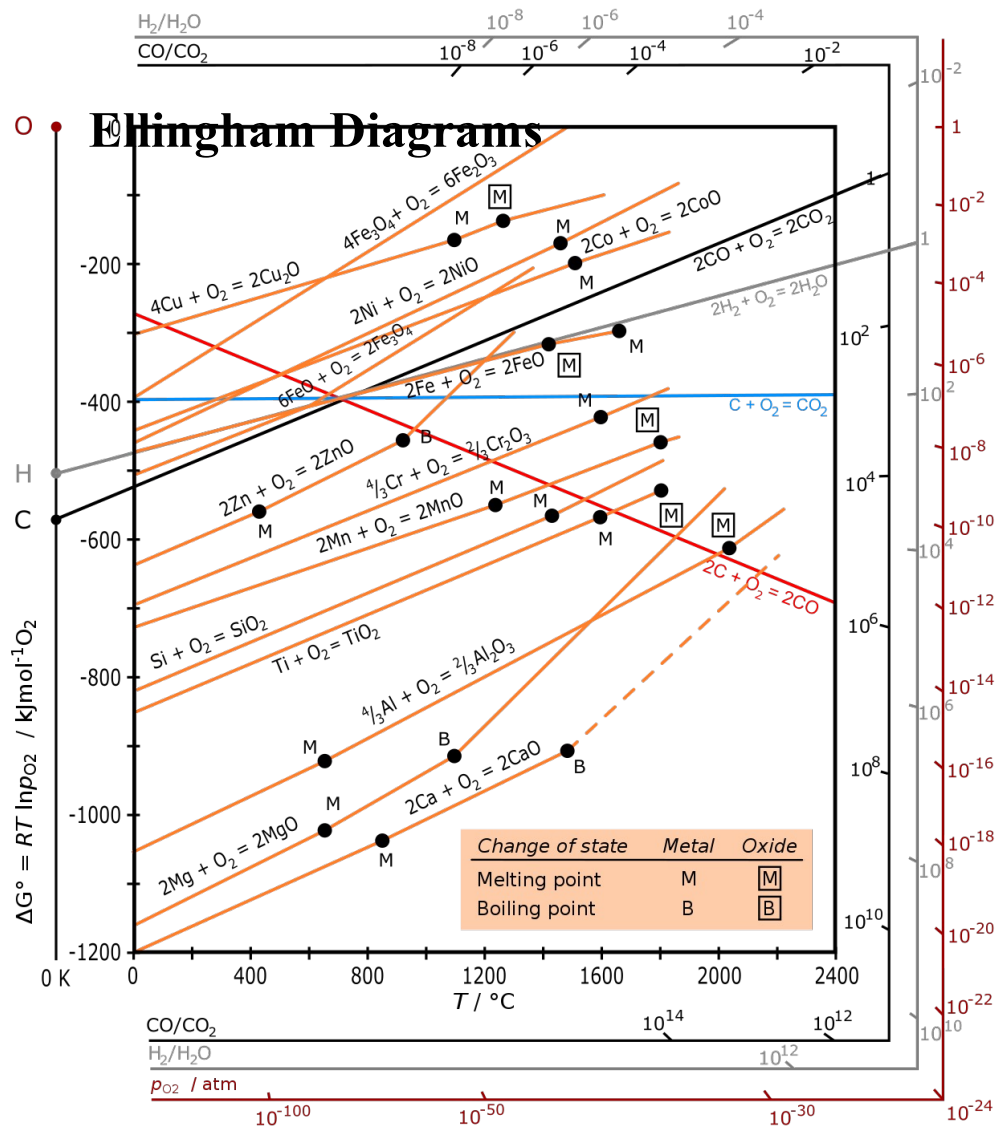
For a reaction
 $\Delta G = \Delta H - T \Delta S$

Gas has more entropy
 than solid

ΔH positive, ΔS negative
 if moles of gas decrease
 A line in ΔG vs T plot
 with positive slope

Reactions that increase
 the moles of gas have
 negative slope

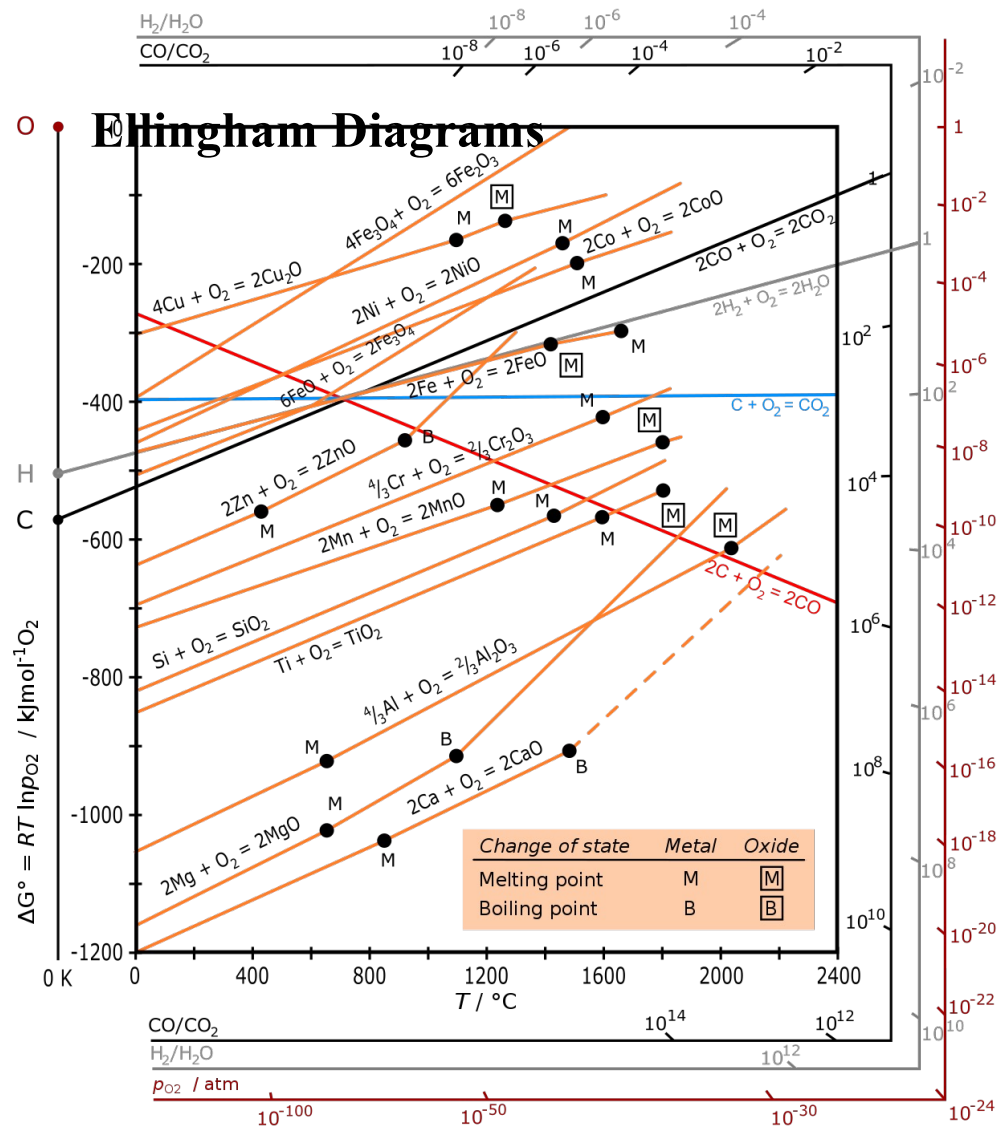
No change in moles of
 gas a flat slope



p_{O_2} is 1 atm

Reactions with one mole of O_2

1. Determine the relative ease of reducing a given metallic oxide to metal
2. Determine the partial pressure of oxygen that is in equilibrium with a metal oxide at a given temperature
3. Determine the ratio of carbon monoxide to carbon dioxide that will be able to reduce the oxide to metal at a given temperature.



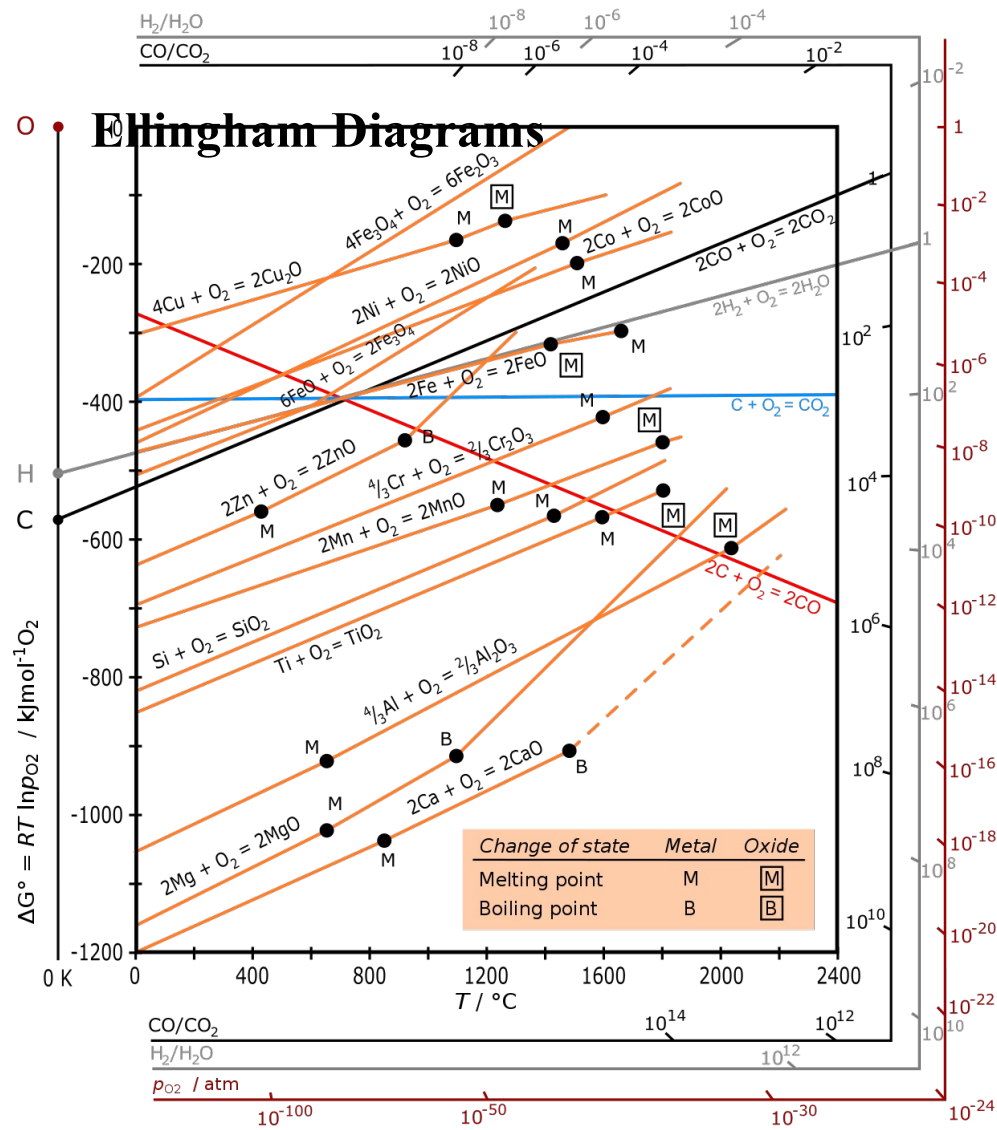
1. Ease of Reduction

Top are most easily reduced

If the curve is below, it will drive the higher curve to reduction (reverse)

High temperatures are needed to reduce iron oxide with carbon (coke)

Magnesothermal reduction, use magnesium metal to reduce titania or silica to titanium metal or silica metal

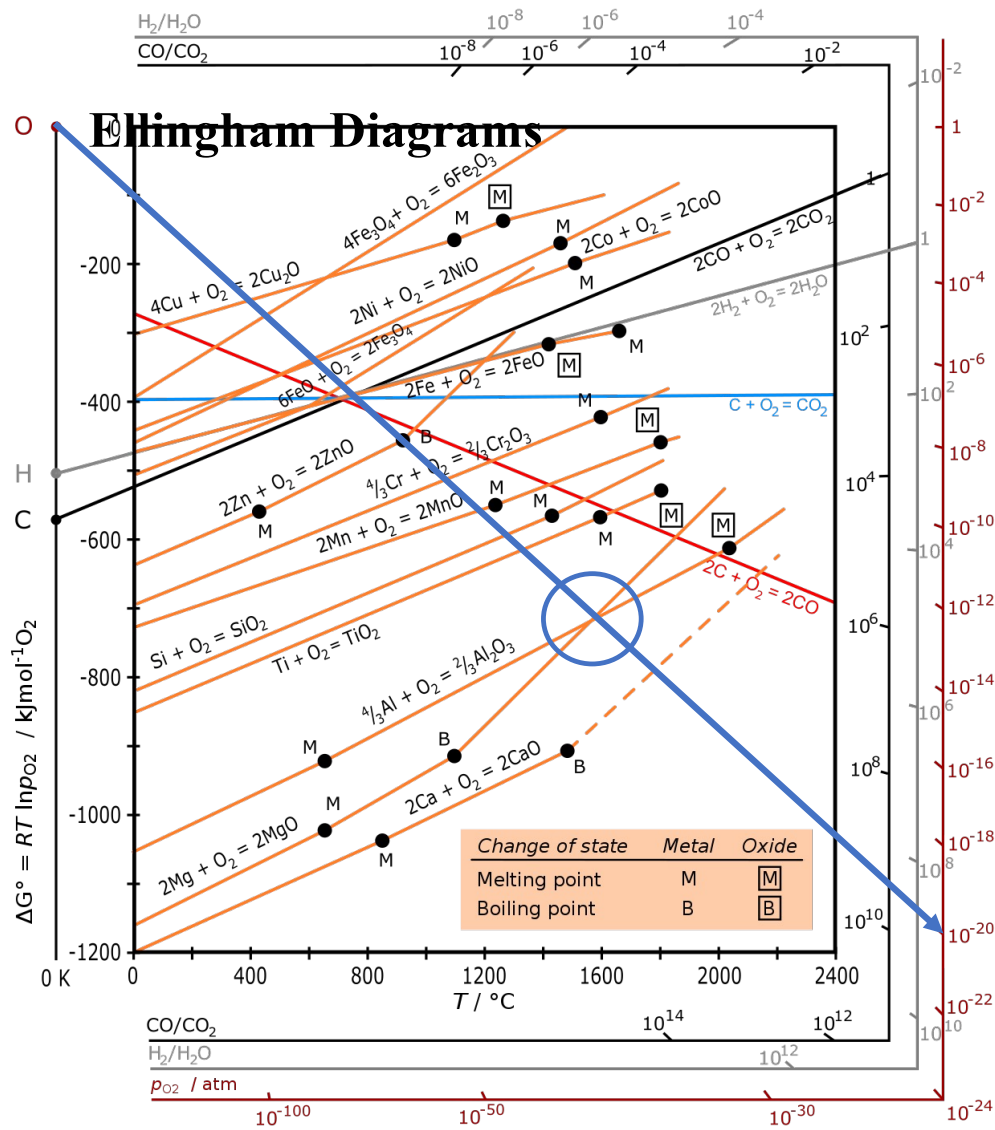


2. Equilibrium O₂ Partial Pressure

Red P_{O₂} scale

Partial pressure of 10⁻²⁰ atm of O₂

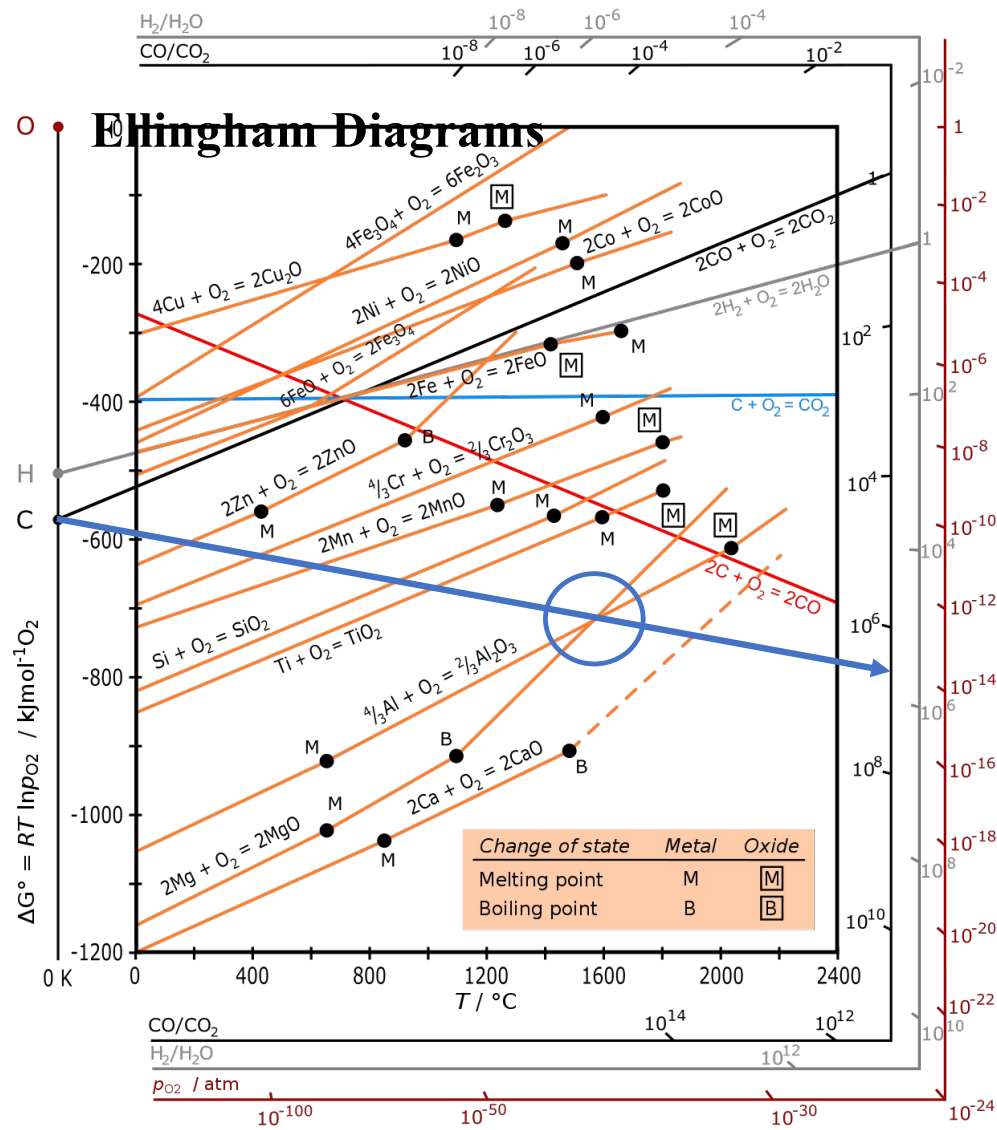
Above will oxidize aluminum at 1600°C
below will reduce



3. Ratio of CO/CO₂ Needed for Reduction with Carbon

To reduce an oxide, you need a minimum CO/CO₂ ratio

To reduce Al at 1600°C you need a CO/CO₂ ratio greater than 5x10⁷



Ellingham Diagrams

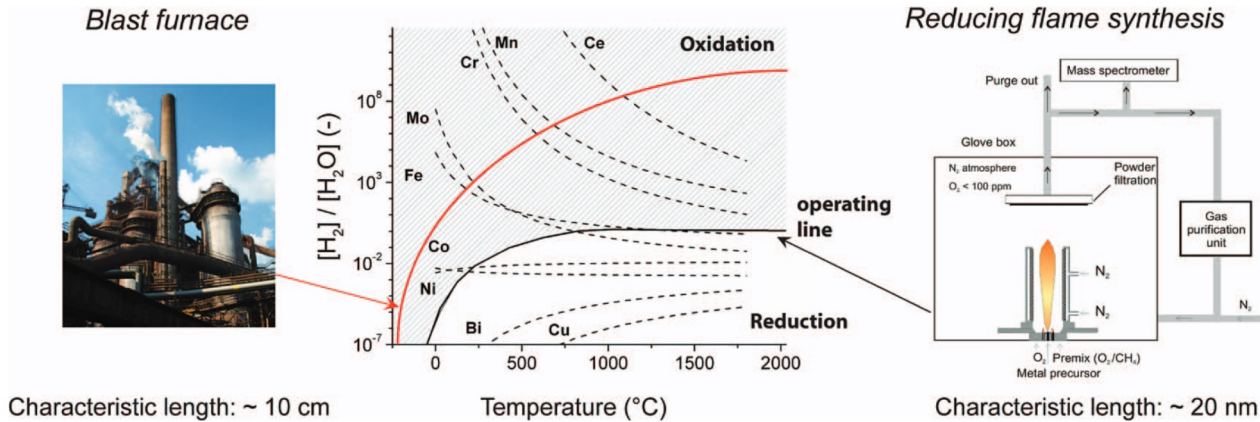


FIG. 5. Thermodynamic calculations in the form of an Ellingham diagram allow discussions on accessible alloys and metals. The lines which lie below the flame process operating line indicate accessible metals at the corresponding temperature (copper, cobalt, nickel, and iron above 1500°C). Others, such as cerium, manganese are not accessible in the current CO/H₂ system.

Aerosol Science and Technology, 44:161–172, 2010
 Copyright © American Association for Aerosol Research
 ISSN: 0278-6826 print / 1521-7388 online
 DOI: 10.1080/02786820903449665

Chemical Aerosol Engineering as a Novel Tool for Material Science: From Oxides to Salt and Metal Nanoparticles

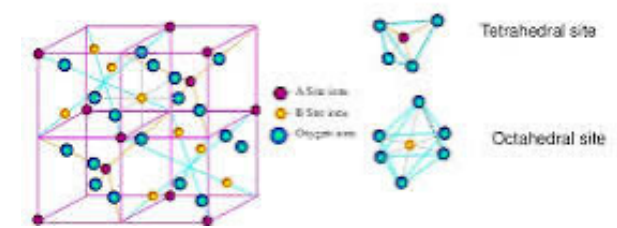
Evangelos K. Athanassiou, Robert N. Grass, and Wendelin J. Stark
Institute for Chemical and Bioengineering, ETH Zurich, Zurich, Switzerland

Relative magnitude of heat of formation from elements, oxides, heat of fusion, heat of transition

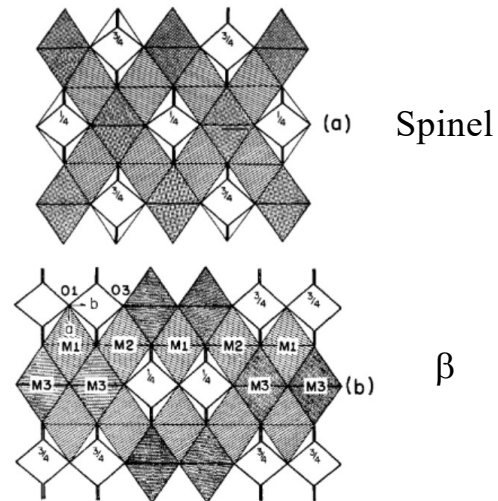
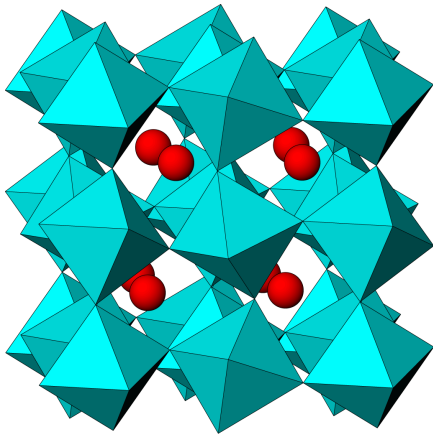
Table 7.1 Magnitudes of enthalpies of various reactions of a ternary oxide using Mg_2SiO_4 as an example (after Navrotsky [1]).

$2\text{Mg}(s) + \text{Si}(s) + 2\text{O}_2(g) = \text{Mg}_2\text{SiO}_4$ (olivine)	$-2170.41 \text{ kJ mol}^{-1}$
$2\text{MgO} + \text{SiO}_2(s) = \text{Mg}_2\text{SiO}_4$ (olivine)	$-56.61 \text{ kJ mol}^{-1}$
Mg_2SiO_4 (olivine) = Mg_2SiO_4 (liq.)	114 kJ mol^{-1}
Mg_2SiO_4 (olivine) = Mg_2SiO_4 (β)	29.9 kJ mol^{-1}
Mg_2SiO_4 (β) = Mg_2SiO_4 (spinel)	9.1 kJ mol^{-1}

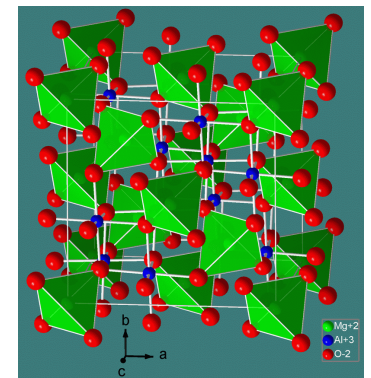
Crystal structure of Spinel Ferrite



Olivine



Spinel



Heats of formation for various titanium oxides

Values are almost identical

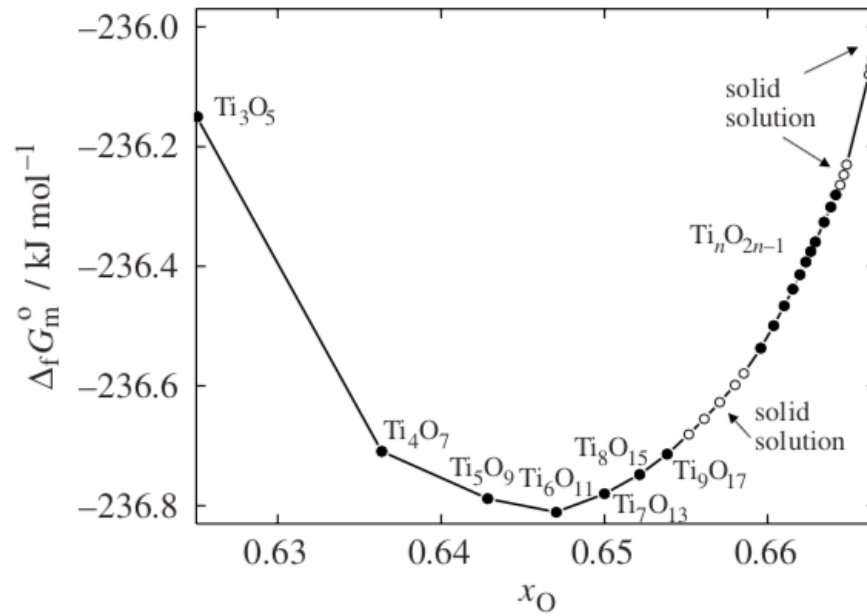
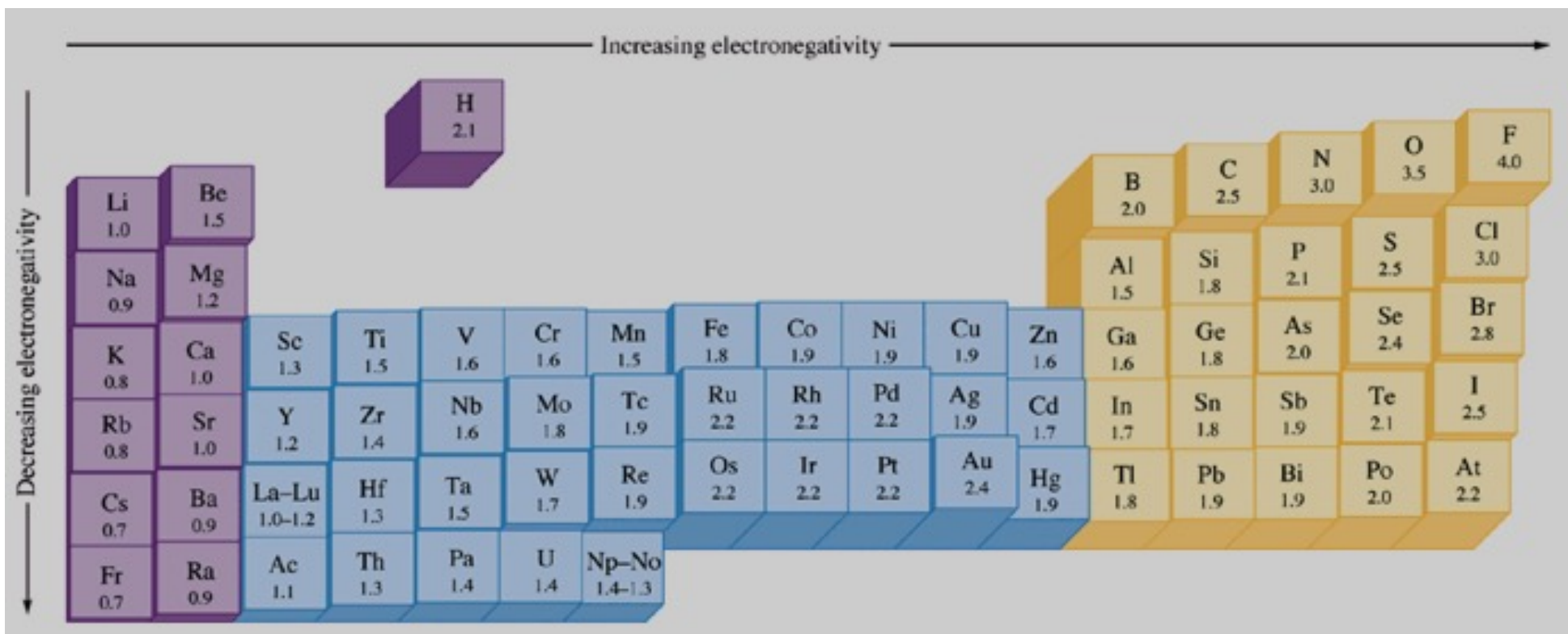


Figure 7.1 The Gibbs energies of formation of stoichiometric and non-stoichiometric compounds in the system Ti_3O_5 – TiO_2 [4]. Composition given as mole fraction O.

Electronegativity, the ability of an atom to attract electrons in a bond

Linus Pauling



Factors involved in the heat of formation: electronegativity and atomic size

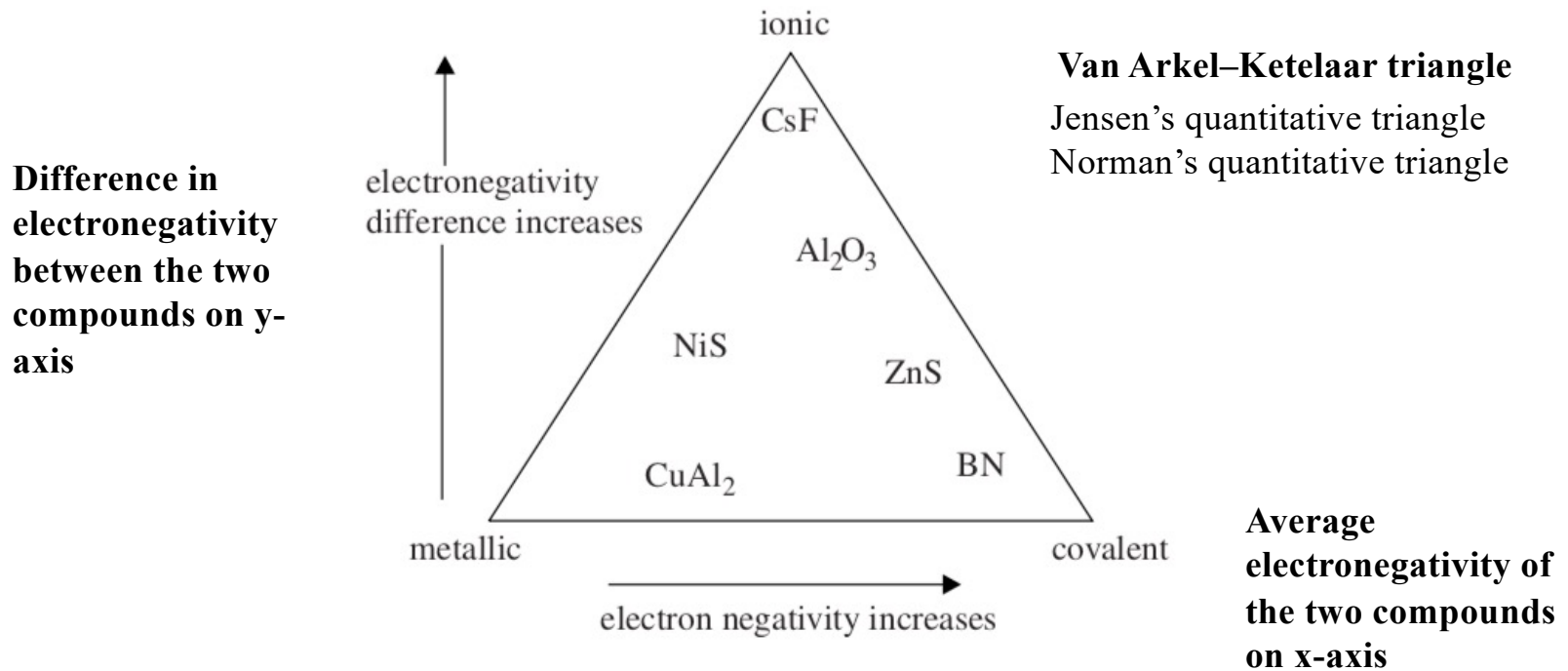


Figure 7.2 Schematic categorization of bonding in solids.

Energetics of compound formation

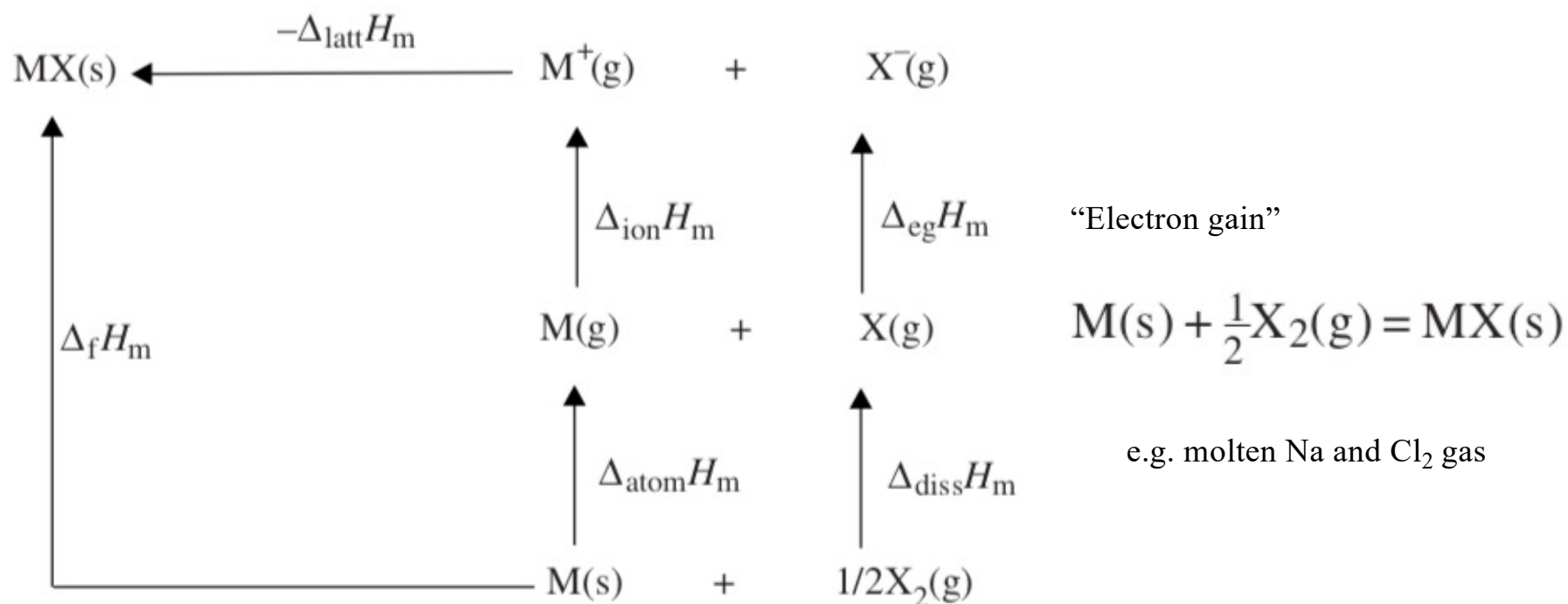


Figure 7.3 Thermodynamic cycle for the formation of MX(s).

Energetics of compound formation

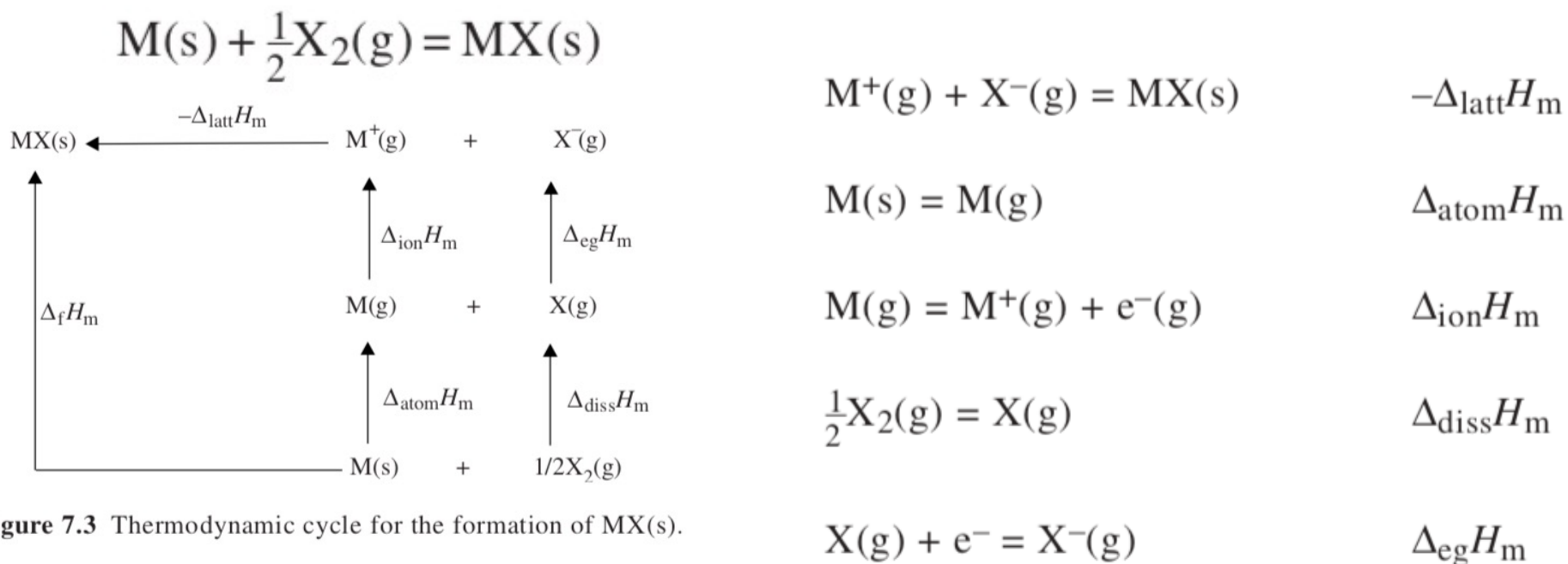


Figure 7.3 Thermodynamic cycle for the formation of MX(s).

$$\Delta_f H_m(MX) = -\Delta_{\text{latt}}H_m + \Delta_{\text{atom}}H_m + \Delta_{\text{ion}}H_m + \Delta_{\text{diss}}H_m + \Delta_{\text{eg}}H_m$$

Energetics of compound formation



$$\Delta_{\text{latt}}H_{\text{m}} = \Phi_{\text{electrostatic}} + \Phi_{\text{repulsion}} + \Phi_{\text{dispersion}} + \Phi_{\text{polarization}} + \Phi_{\text{crystal field}}$$

Electrostatic attraction +-
Electron electron repulsion

Electron electron repulsion

Van der Waals or dispersion (d+ makes d- leads to net attraction)

Polarization (shifting within compound of electrons)

Crystal field effects

$$\Delta_{\text{latt}}H_m = \Phi_{\text{electrostatic}} + \Phi_{\text{repulsion}} + \Phi_{\text{dispersion}} + \Phi_{\text{polarization}} + \Phi_{\text{crystal field}}$$

Electrostatic interactions in NaCl

$$6 \frac{e^2 q_M q_X}{r_{MX}}$$

Nearest neighbors of Na⁺ and Cl⁻

$$-12 \frac{e^2 q_M q_X}{\sqrt{2} r_{MX}}$$

Repulsive cationic terms, second nearest neighbors

$$8 \frac{e^2 q_M q_X}{\sqrt{3} r_{MX}}$$

Third nearest neighbors, attraction between M⁺ and X⁻

$$\Phi = \frac{e^2 q_M q_X}{r_{MX}} \left(6 - \frac{12}{\sqrt{2}} + \frac{8}{\sqrt{3}} - \frac{6}{\sqrt{4}} + \dots \right)$$

Generally:

$$\Phi_{\text{electrostatic}} = \frac{N M e^2 q_M q_X}{r_{MX}}$$

M is the Madelung constant

$$\Delta_{\text{latt}}H_m = \Phi_{\text{electrostatic}} + \Phi_{\text{repulsion}} + \Phi_{\text{dispersion}} + \Phi_{\text{polarization}} + \Phi_{\text{crystal field}}$$

Repulsion and Dispersion Terms

Leonard-Jones (6-12) Potential

$$V_{\text{LJ}}(r) = \frac{A}{r^{12}} - \frac{B}{r^6}$$

12 is repulsive since $dE/dr = F$ is positive (guessed)
6 is van der Waals attractive force (calculated)

Buckingham Potential

$$\Phi_{12}(r) = A \exp(-Br) - \frac{C}{r^6}$$

Exponential term works better for ceramics

$$\Delta_f H_m(MX) = -\Delta_{\text{lattice}} H_m + \Delta_{\text{atom}} H_m + \Delta_{\text{ion}} H_m + \Delta_{\text{diss}} H_m + \Delta_{\text{eg}} H_m \quad (7.8)$$

Trends in Enthalpy of Formation Alkali

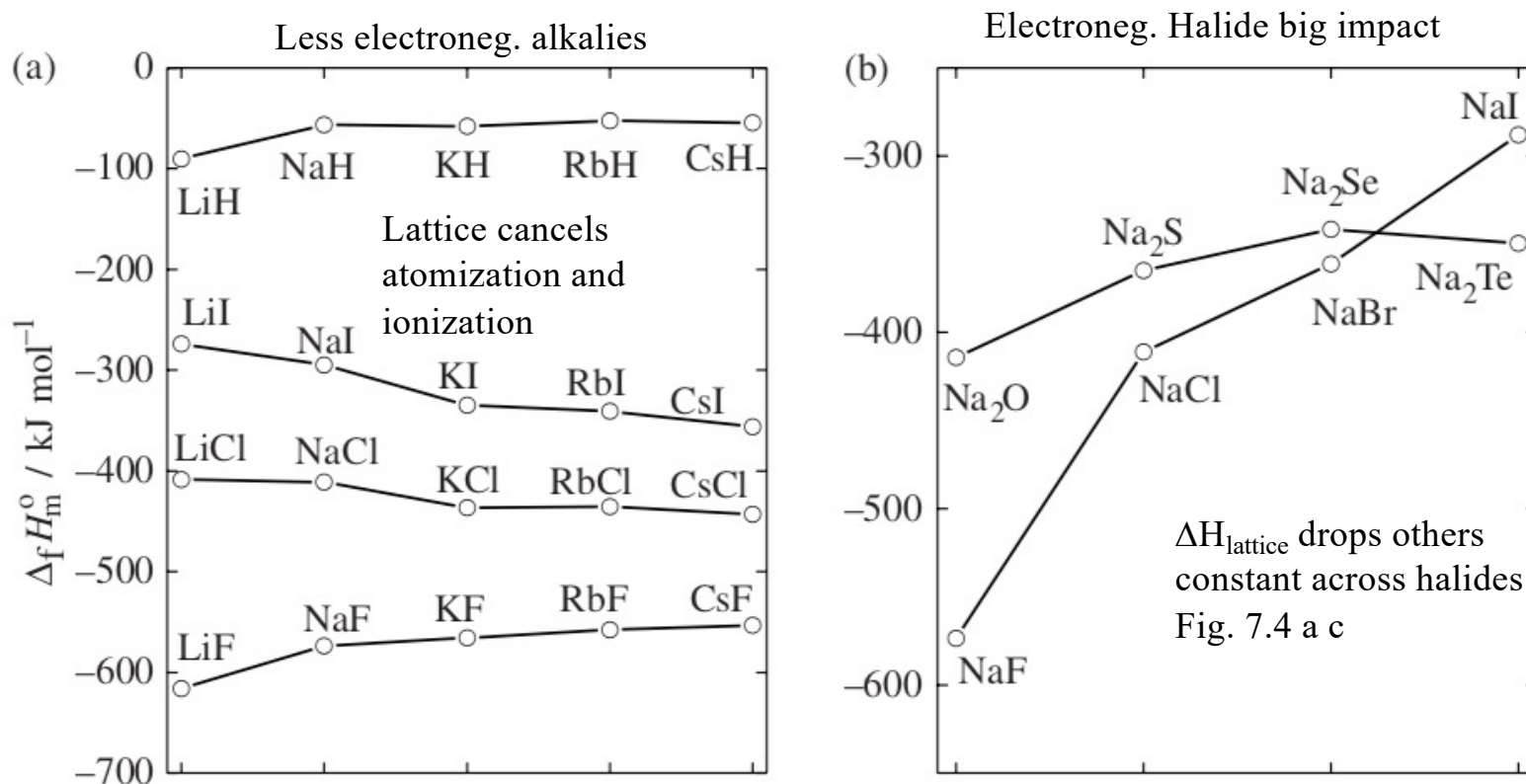
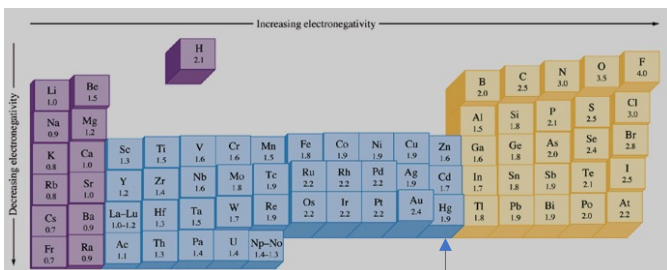


Figure 7.5 Enthalpy of formation of binary compounds of the alkali metals.



“Extra electrons (12) are not screening the nuclear charge effectively, resulting in a much **higher ionization enthalpy** for the group 12 elements and a **less negative enthalpy of formation** for the group 12 compounds compared with the group 2 compounds.” (book)

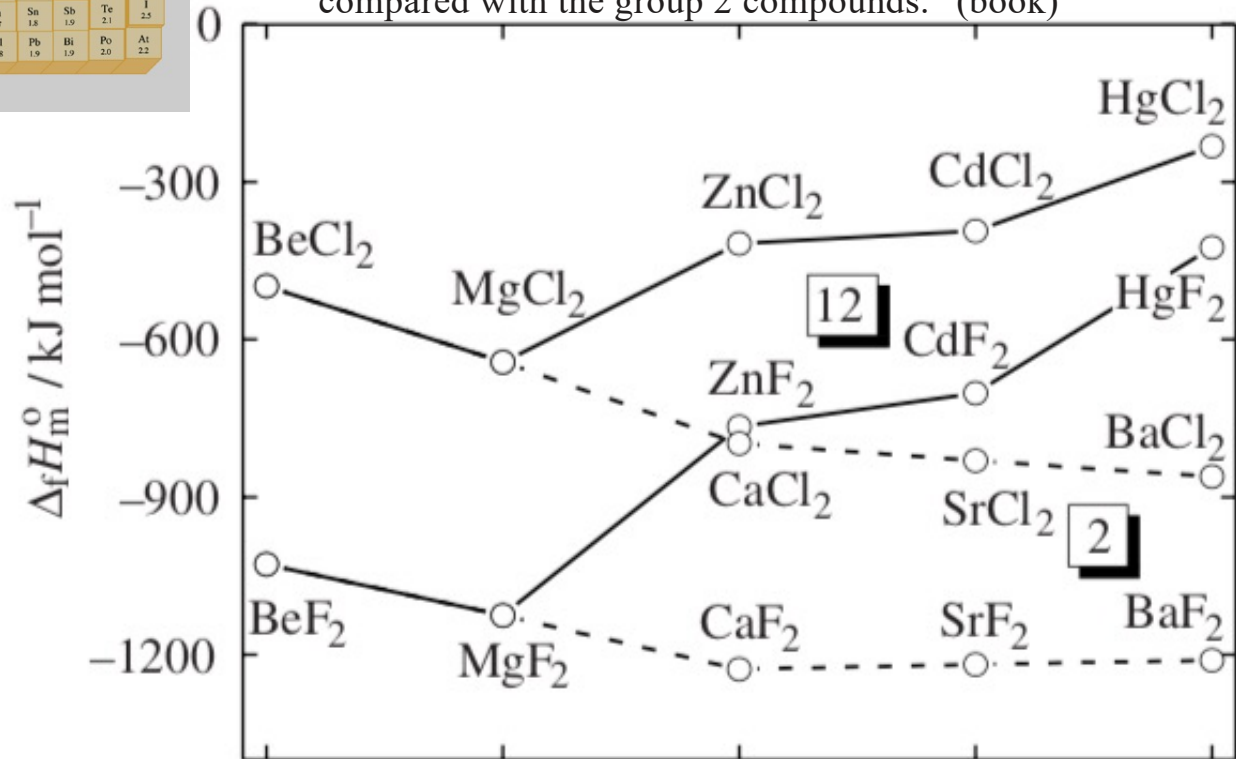


Figure 7.6 Enthalpy of formation of group 2 and 12 dichlorides and difluorides.

Transition Metal Enthalpy of Formation

$$\Delta_{\text{latt}}H_{\text{m}} = \Phi_{\text{electrostatic}} + \Phi_{\text{repulsion}} + \Phi_{\text{dispersion}} + \Phi_{\text{polarization}} \\ + \Phi_{\text{crystal field}}$$

Crystal Field Theory (CFT):

This theory explains how the arrangement of ligands around a central metal ion splits the d orbitals into different energy levels, depending on the geometry of the complex.

V·T·E **Blocks in the periodic table** [hide]

Group	1	2	3	4	5	6	7	8	9	10	11	12	13	14	15	16	17	18	
↓ Period																			
1	1 H																	2 He	
2	3 Li	4 Be											5 B	6 C	7 N	8 O	9 F	10 Ne	
3	11 Na	12 Mg											13 Al	14 Si	15 P	16 S	17 Cl	18 Ar	
4	19 K	20 Ca	21 Sc	22 Ti	23 V	24 Cr	25 Mn	26 Fe	27 Co	28 Ni	29 Cu	30 Zn	31 Ga	32 Ge	33 As	34 Se	35 Br	36 Kr	
5	37 Rb	38 Sr	39 Y	40 Zr	41 Nb	42 Mo	43 Tc	44 Ru	45 Rh	46 Pd	47 Ag	48 Cd	49 In	50 Sn	51 Sb	52 Te	53 I	54 Xe	
6	55 Cs	56 Ba	57 La	*	72 Hf	73 Ta	74 W	75 Re	76 Os	77 Ir	78 Pt	79 Au	80 Hg	81 Tl	82 Pb	83 Bi	84 Po	85 At	86 Rn
7	87 Fr	88 Ra	89 Ac	**	104 Rf	105 Db	106 Sg	107 Bh	108 Hs	109 Mt	110 Ds	111 Rg	112 Cn	113 Nh	114 Fl	115 Mc	116 Lv	117 Ts	118 Og
				*	58 Ce	59 Pr	60 Nd	61 Pm	62 Sm	63 Eu	64 Gd	65 Tb	66 Dy	67 Ho	68 Er	69 Tm	70 Yb	71 Lu	
				**	90 Th	91 Pa	92 U	93 Np	94 Pu	95 Am	96 Cm	97 Bk	98 Cf	99 Es	100 Fm	101 Md	102 No	103 Lr	

Basic (at low oxidation state) Transition Metals Acidic (at high oxidation state)

Basic s-orbitals 2 valence electrons (more basic to right) d-orbitals 10 valence electrons Acidic p-orbitals 6 valence electrons (more acidic to right)

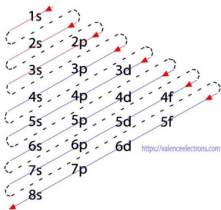
f-orbitals 14 valence electrons

* Primordial ** From decay Synthetic Border shows natural occurrence of the element

Background color shows the block of the periodic table

Electron Configuration in the Aufbau principle

s = 2
 p = 6
 d = 10
 f = 14

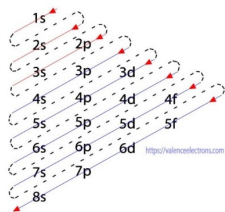


Hybridization schemes for the σ -bonding frameworks of different geometrical configurations

Coordination number	Arrangement of donor atoms	Orbitals hybridized	Hybrid orbital description	Example
2	Linear	s, p_z	sp	$[\text{Ag}(\text{NH}_3)_2]^+$
3	Trigonal planar	s, p_x, p_y	sp^2	$[\text{HgI}_3]^-$
4	Tetrahedral	s, p_x, p_y, p_z	sp^3	$[\text{FeBr}_4]^{2-}$
4	Square planar	$s, p_x, p_y, d_{x^2-y^2}$	$sp^2 d$	$[\text{Ni}(\text{CN})_4]^{2-}$
5	Trigonal bipyramidal	$s, p_x, p_y, p_z, d_{z^2}$	$sp^3 d$	$[\text{CuCl}_5]^{3-}$
5	Square-based pyramidal	$s, p_x, p_y, p_z, d_{x^2-y^2}$	$sp^3 d$	$[\text{Ni}(\text{CN})_5]^{3-}$
6	Octahedral	$s, p_x, p_y, p_z, d_{z^2}, d_{x^2-y^2}$	$sp^3 d^2$	$[\text{Co}(\text{NH}_3)_6]^{3+}$
6	Trigonal prismatic	$s, d_{xy}, d_{yz}, d_{xz}, d_{z^2}, d_{x^2-y^2}$ or $s, p_x, p_y, p_z, d_{xz}, d_{yz}$	sd^5 or $sp^3 d^2$	$[\text{ZrMe}_6]^{2-}$
7	Pentagonal bipyramidal	$s, p_x, p_y, p_z, d_{xy}, d_{x^2-y^2}, d_{z^2}$	$sp^3 d^3$	$[\text{V}(\text{CN})_7]^{4-}$
7	Monocapped trigonal prismatic	$s, p_x, p_y, p_z, d_{xy}, d_{xz}, d_{z^2}$	$sp^3 d^3$	$[\text{NbF}_7]^{2-}$
8	Cubic	$s, p_x, p_y, p_z, d_{xy}, d_{xz}, d_{yz}, f_{xyz}$	$sp^3 d^3 f$	$[\text{PaF}_8]^{3-}$
8	Dodecahedral	$s, p_x, p_y, p_z, d_{z^2}, d_{xy}, d_{xz}, d_{yz}$	$sp^3 d^4$	$[\text{Mo}(\text{CN})_8]^{4-}$
8	Square antiprismatic	$s, p_x, p_y, p_z, d_{xy}, d_{xz}, d_{yz}, d_{x^2-y^2}$	$sp^3 d^4$	$[\text{TaF}_8]^{3-}$
9	Tricapped trigonal prismatic	$s, p_x, p_y, p_z, d_{xy}, d_{xz}, d_{yz}, d_{z^2}, d_{x^2-y^2}$	$sp^3 d^5$	$[\text{ReH}_9]^{2-}$

Electron Configuration in the Aufbau principle

S = 2
p = 6
d = 10
f = 14



f-or
14
electrons

Depending on the crystallographic environment the d-orbital energies split This impacts the Enthalpy of Formation

[https://chem.libretexts.org/Bookshelves/Inorganic_Chemistry/Supplemental_Modules_and_Web_sites_\(Inorganic_Chemistry\)/Crystal_Field_Theory/Crystal_Field_Theory](https://chem.libretexts.org/Bookshelves/Inorganic_Chemistry/Supplemental_Modules_and_Web_sites_(Inorganic_Chemistry)/Crystal_Field_Theory/Crystal_Field_Theory)

Crystal Field Theory

$$E \propto \frac{q_1 q_2}{r}$$

- E the bond energy between the charges and
- q_1 and q_2 are the charges of the interacting ions and
- r is the distance separating them.

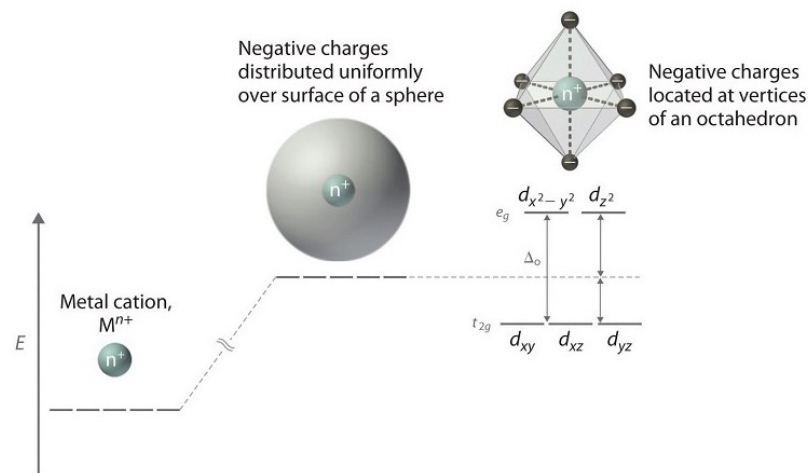
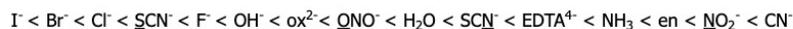


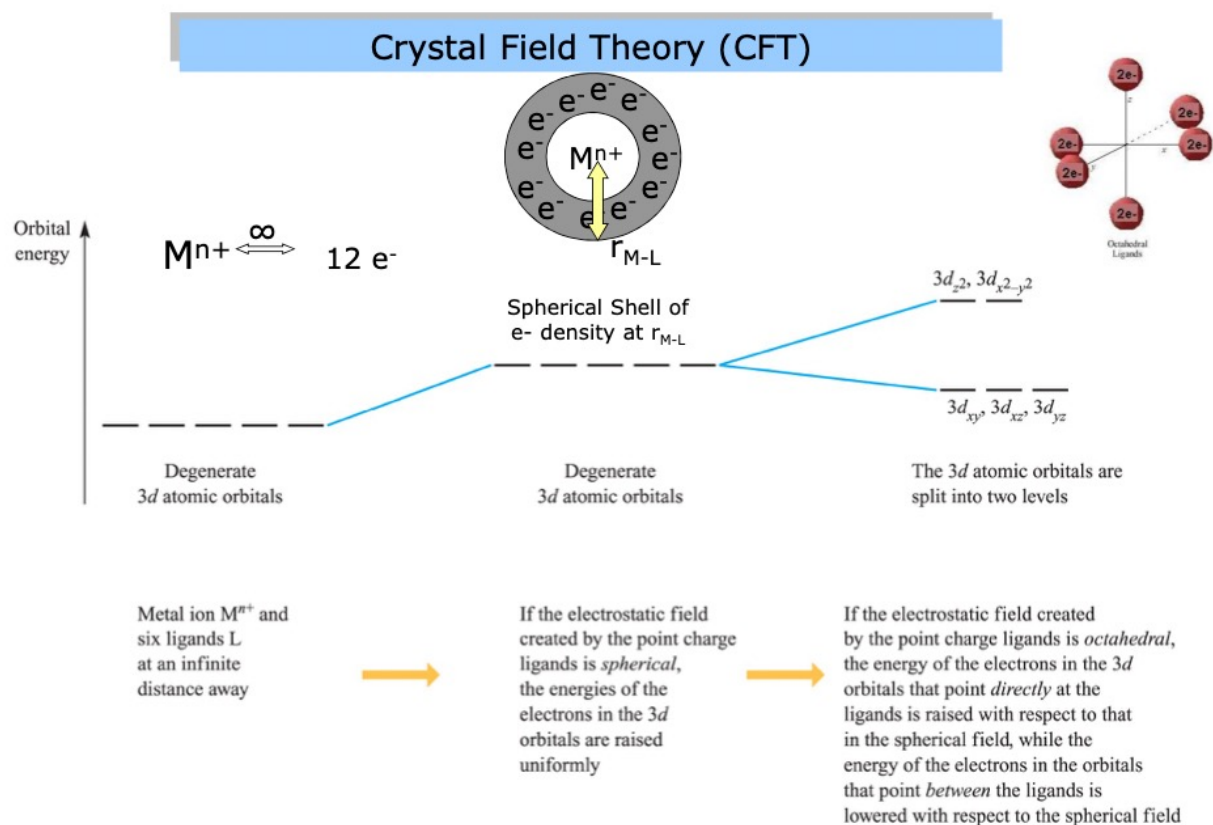
Figure 1: Distributing a charge of -6 uniformly over a spherical surface surrounding a metal ion causes the energy of all five d orbitals to increase due to electrostatic repulsions, but the five d orbitals remain degenerate. Placing a charge of -1 at each vertex of an octahedron causes the d orbitals to split into two groups with different energies: the $d_{x^2-y^2}$ and d_{z^2} orbitals increase in energy, while the d_{xy} , d_{xz} , and d_{yz} orbitals decrease in energy. The average energy of the five d orbitals is the same as for a spherical distribution of a -6 charge, however. Attractive electrostatic interactions between the negatively charged ligands and the positively charged metal ion (far right) cause all five d orbitals to decrease in energy but does not affect the splittings of the orbitals. The two e_g orbitals point directly at the six negatively charged ligands, which increases their energy compared with a spherical distribution of negative charge. In contrast, the three t_{2g} orbitals point between the negatively charged ligands, which decreases their energy compared with a spherical distribution of charge.

larger the splitting. Ligands are classified as strong or weak based on the spectrochemical series:



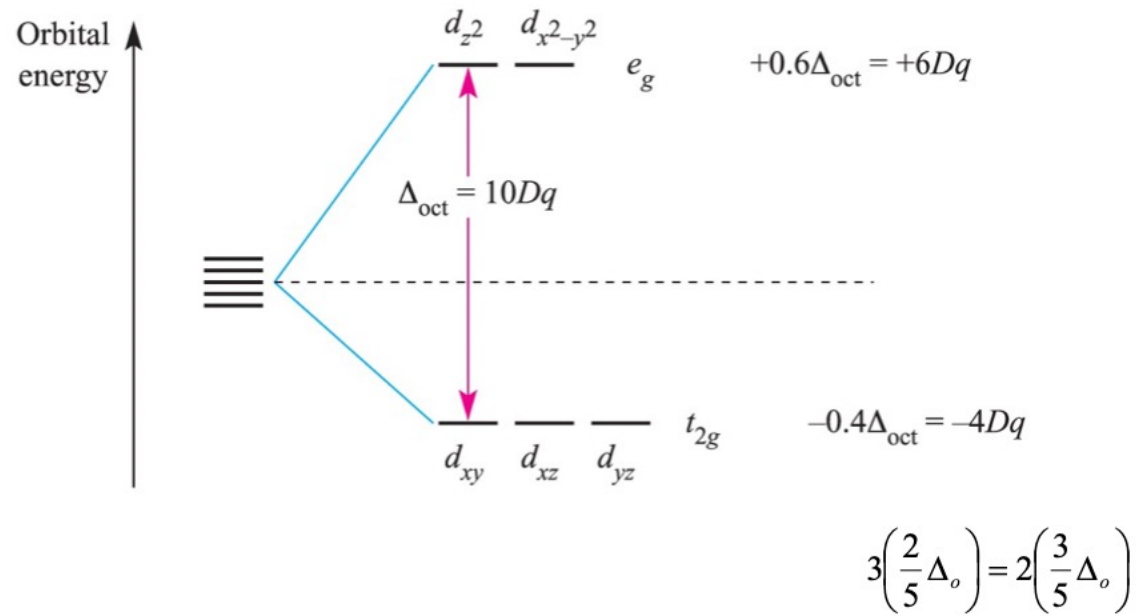
Note that SCN^- and NO_2^- ligands are represented twice in the above spectrochemical series since there are two different Lewis base sites (e.g., free electron pairs to share) on each ligand (e.g., for the SCN^- ligand, the electron pair on the sulfur or the nitrogen can form the **coordinate covalent bond** to a metal). The specific atom that binds in such ligands is underlined.

Depending on the crystallographic environment the d-orbital energies split

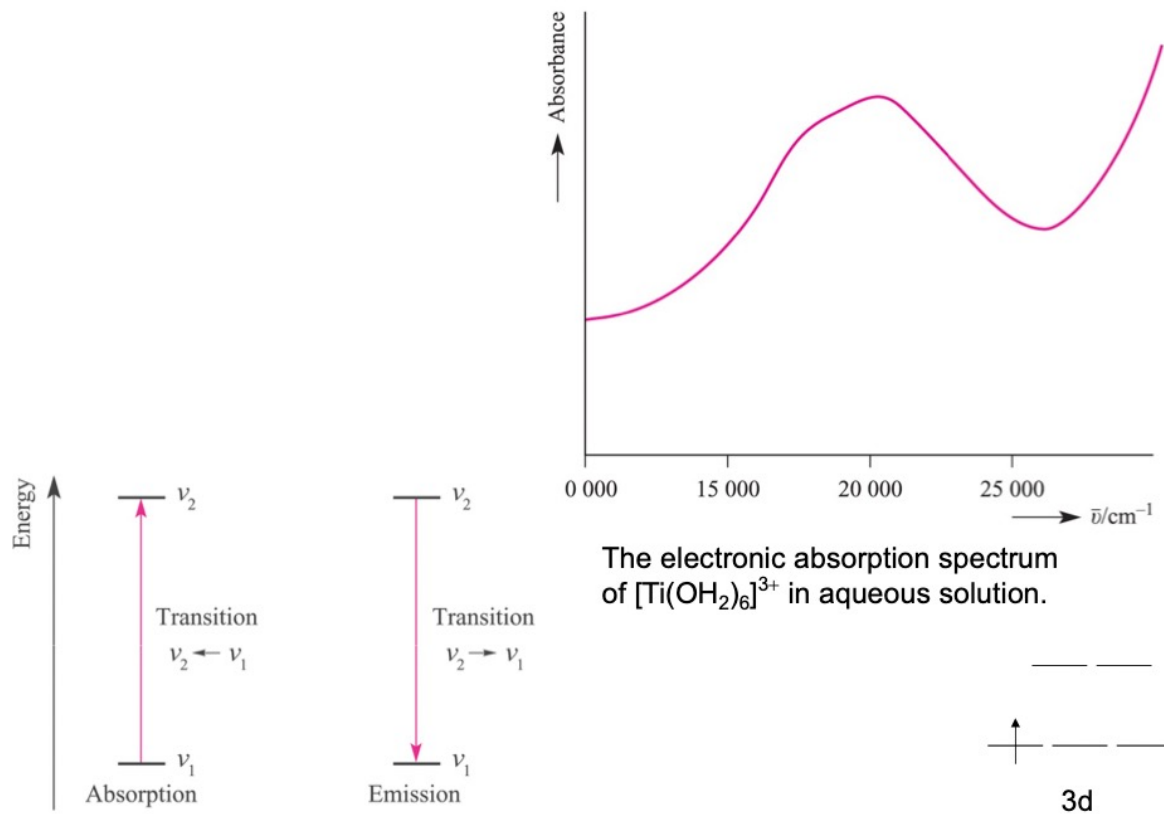


Depending on the crystallographic environment the d-orbital energies split

Crystal Field Stabilization Energy (CFSE)



Depending on the crystallographic environment the d-orbital energies split



Complex	Δ / cm^{-1}	Complex	Δ / cm^{-1}
$[\text{TiF}_6]^{3-}$	17 000	$[\text{Fe}(\text{ox})_3]^{3-}$	14 100
$[\text{Ti}(\text{OH}_2)_6]^{3+}$	20 300	$[\text{Fe}(\text{CN})_6]^{3-}$	35 000
$[\text{V}(\text{OH}_2)_6]^{3+}$	17 850	$[\text{Fe}(\text{CN})_6]^{4-}$	33 800
$[\text{V}(\text{OH}_2)_6]^{2+}$	12 400	$[\text{CoF}_6]^{3-}$	13 100
$[\text{CrF}_6]^{3-}$	15 000	$[\text{Co}(\text{NH}_3)_6]^{3+}$	22 900
$[\text{Cr}(\text{OH}_2)_6]^{3+}$	17 400	$[\text{Co}(\text{NH}_3)_6]^{2+}$	10 200
$[\text{Cr}(\text{OH}_2)_6]^{2+}$	14 100	$[\text{Co}(\text{en})_3]^{3+}$	24 000
$[\text{Cr}(\text{NH}_3)_6]^{3+}$	21 600	$[\text{Co}(\text{OH}_2)_6]^{3+}$	18 200
$[\text{Cr}(\text{CN})_6]^{3-}$	26 600	$[\text{Co}(\text{OH}_2)_6]^{2+}$	9 300
$[\text{MnF}_6]^{2-}$	21 800	$[\text{Ni}(\text{OH}_2)_6]^{2+}$	8 500
$[\text{Fe}(\text{OH}_2)_6]^{3+}$	13 700	$[\text{Ni}(\text{NH}_3)_6]^{2+}$	10 800
$[\text{Fe}(\text{OH}_2)_6]^{2+}$	9 400	$[\text{Ni}(\text{en})_3]^{2+}$	11 500

Values of Δ_{oct} for some *d*-block metal complexes.

Depending on the crystallographic environment the d-orbital energies split This impacts the Enthalpy of Formation

[https://chem.libretexts.org/Bookshelves/Inorganic_Chemistry/Supplemental_Modules_and_Web_sites_\(Inorganic_Chemistry\)/Crystal_Field_Theory/Crystal_Field_Theory](https://chem.libretexts.org/Bookshelves/Inorganic_Chemistry/Supplemental_Modules_and_Web_sites_(Inorganic_Chemistry)/Crystal_Field_Theory/Crystal_Field_Theory)

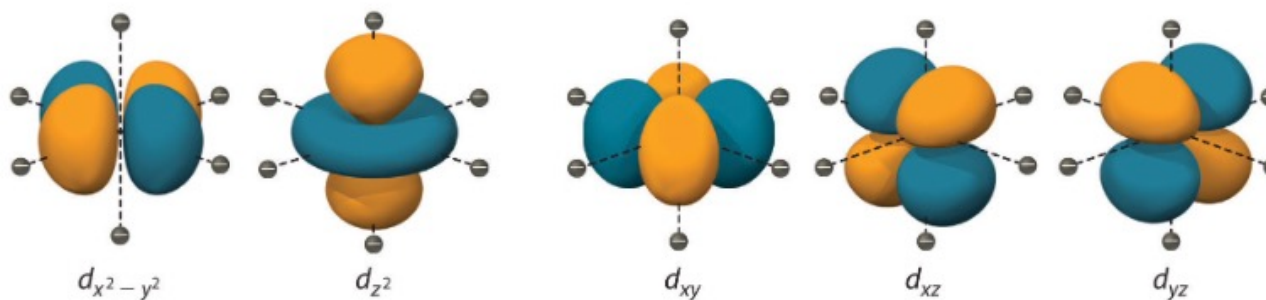


Figure 3: Spatial arrangement of ligands in the an octahedral ligand field with respect to the five d-orbitals.

- d_{xy} : lobes lie in-between the x and the y axes.
- d_{xz} : lobes lie in-between the x and the z axes.
- d_{yz} : lobes lie in-between the y and the z axes.
- $d_{x^2-y^2}$: lobes lie on the x and y axes.
- d_{z^2} : there are two lobes on the z axes and there is a donut shape ring that lies on the xy plane around the other two lobes.

Depending on the crystallographic environment the d-orbital energies split This impacts the Enthalpy of Formation

[https://chem.libretexts.org/Bookshelves/Inorganic_Chemistry/Supplemental_Modules_and_Web sites_\(Inorganic_Chemistry\)/Crystal_Field_Theory/Crystal_Field_Theory](https://chem.libretexts.org/Bookshelves/Inorganic_Chemistry/Supplemental_Modules_and_Web_sites_(Inorganic_Chemistry)/Crystal_Field_Theory/Crystal_Field_Theory)

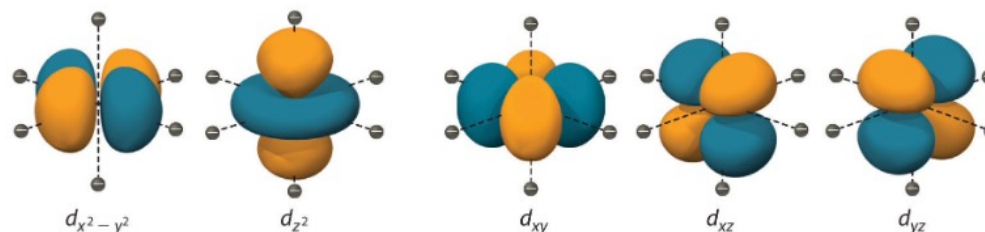


Figure 3: Spatial arrangement of ligands in the an octahedral ligand field with respect to the five d-orbitals.

Octahedral Complexes

In an **octahedral complex**, there are six ligands attached to the central transition metal. The d-orbital splits into two different levels (Figure 4). The bottom three energy levels are named d_{xy} , d_{xz} , and d_{yz} (collectively referred to as t_{2g}). The two upper energy levels are named $d_{x^2-y^2}$, and d_{z^2} (collectively referred to as e_g).

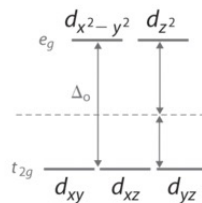
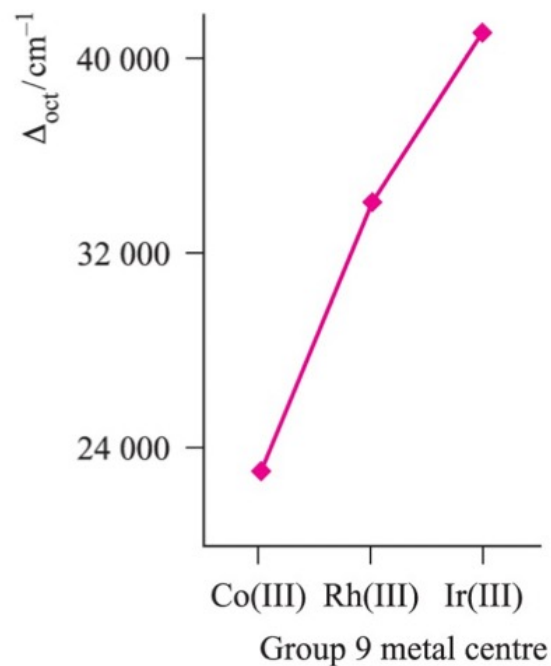


Figure 4.

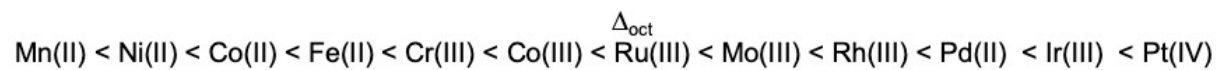
The reason they split is because of the electrostatic interactions between the electrons of the ligand and the lobes of the d-orbital. In an octahedral, the electrons are attracted to the axes. Any orbital that has a lobe on the axes moves to a higher energy level. This means that in an octahedral, the energy levels of e_g are higher ($0.6\Delta_o$) while t_{2g} is lower ($0.4\Delta_o$). The distance that the electrons have to move from t_{2g} from e_g and it dictates the energy that the complex will absorb from white light, which will determine the **color**. Whether the complex is **paramagnetic or diamagnetic** will be determined by the spin state. If there are unpaired electrons, the complex is paramagnetic; if all electrons are paired, the complex is diamagnetic.

Depending on the crystallographic environment the d-orbital energies split



The trend in values of Δ_{oct} for the complexes $[\text{M}(\text{NH}_3)_6]^{3+}$ where M = Co, Rh, Ir.

Field strength increases as one proceeds down a column.



Complex	Δ / cm^{-1}	Complex	Δ / cm^{-1}
$[\text{TiF}_6]^{3-}$	17 000	$[\text{Fe}(\text{ox})_3]^{3-}$	14 100
$[\text{Ti}(\text{OH}_2)_6]^{3+}$	20 300	$[\text{Fe}(\text{CN})_6]^{3-}$	35 000
$[\text{V}(\text{OH}_2)_6]^{3+}$	17 850	$[\text{Fe}(\text{CN})_6]^{4-}$	33 800
$[\text{V}(\text{OH}_2)_6]^{2+}$	12 400	$[\text{CoF}_6]^{3-}$	13 100
$[\text{CrF}_6]^{3-}$	15 000	$[\text{Co}(\text{NH}_3)_6]^{3+}$	22 900
$[\text{Cr}(\text{OH}_2)_6]^{3+}$	17 400	$[\text{Co}(\text{NH}_3)_6]^{2+}$	10 200
$[\text{Cr}(\text{OH}_2)_6]^{2+}$	14 100	$[\text{Co}(\text{en})_3]^{3+}$	24 000
$[\text{Cr}(\text{NH}_3)_6]^{3+}$	21 600	$[\text{Co}(\text{OH}_2)_6]^{3+}$	18 200
$[\text{Cr}(\text{CN})_6]^{3-}$	26 600	$[\text{Co}(\text{OH}_2)_6]^{2+}$	9 300
$[\text{MnF}_6]^{2-}$	21 800	$[\text{Ni}(\text{OH}_2)_6]^{2+}$	8 500
$[\text{Fe}(\text{OH}_2)_6]^{3+}$	13 700	$[\text{Ni}(\text{NH}_3)_6]^{2+}$	10 800
$[\text{Fe}(\text{OH}_2)_6]^{2+}$	9 400	$[\text{Ni}(\text{en})_3]^{2+}$	11 500

plit

Values of Δ_{oct} for some *d*-block metal complexes.

Depending on the crystallographic environment the d-orbital energies split This impacts the Enthalpy of Formation

[https://chem.libretexts.org/Bookshelves/Inorganic_Chemistry/Supplemental_Modules_and_Web sites_\(Inorganic_Chemistry\)/Crystal_Field_Theory/Crystal_Field_Theory](https://chem.libretexts.org/Bookshelves/Inorganic_Chemistry/Supplemental_Modules_and_Web_sites_(Inorganic_Chemistry)/Crystal_Field_Theory/Crystal_Field_Theory)

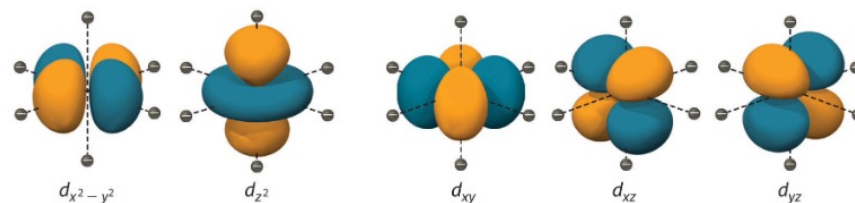


Figure 3: Spatial arrangement of ligands in an octahedral ligand field with respect to the five d-orbitals.

Tetrahedral Complexes

In a tetrahedral complex, there are four ligands attached to the central metal. The d orbitals also split into two different energy levels. The top three consist of the d_{xy} , d_{xz} , and d_{yz} orbitals. The bottom two consist of the $d_{x^2-y^2}$ and d_{z^2} orbitals. The reason for this is due to poor orbital overlap between the metal and the ligand orbitals. The orbitals are directed on the axes, while the ligands are not.

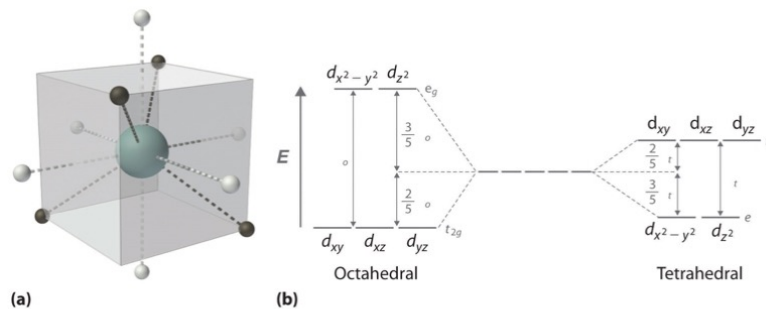


Figure 5: (a) Tetrahedral ligand field surrounding a central transition metal (blue sphere). (b) Splitting of the degenerate d-orbitals (without a ligand field) due to an octahedral ligand field (left diagram) and the tetrahedral field (right diagram).

The difference in the splitting energy is tetrahedral splitting constant (Δ_t), which is less than (Δ_o) for the same ligands:

$$\Delta_t = 0.44 \Delta_o \quad (2)$$

Consequently, Δ_t is typically smaller than the **spin pairing energy**, so tetrahedral complexes are usually **high spin**.

Depending on the crystallographic environment the d-orbital energies split This impacts the Enthalpy of Formation

[https://chem.libretexts.org/Bookshelves/Inorganic_Chemistry/Supplemental_Modules_and_Web_sites_\(Inorganic_Chemistry\)/Crystal_Field_Theory/Crystal_Field_Theory](https://chem.libretexts.org/Bookshelves/Inorganic_Chemistry/Supplemental_Modules_and_Web_sites_(Inorganic_Chemistry)/Crystal_Field_Theory/Crystal_Field_Theory)

Spin Pairing Energy

- The energy needed to pair two electrons in the same orbital, overcoming the natural tendency for electrons to occupy different orbitals with parallel spins (Hund's rule).

•Impact on complex behavior:

- When considering transition metal complexes, the relative magnitude of the spin pairing energy compared to the crystal field splitting energy determines whether a complex will be "high spin" (with many unpaired electrons) or "low spin" (with more paired electrons).

•Paramagnetism and diamagnetism:

- If a complex has unpaired electrons (high spin), it will be paramagnetic, meaning it will be attracted to a magnetic field; if all electrons are paired (low spin), it will be diamagnetic, repelled by a magnetic field.

Depending on the crystallographic environment the d-orbital energies split This impacts the Enthalpy of Formation

[https://chem.libretexts.org/Bookshelves/Inorganic_Chemistry/Supplemental_Modules_and_Web_sites_\(Inorganic_Chemistry\)/Crystal_Field_Theory/Crystal_Field_Theory](https://chem.libretexts.org/Bookshelves/Inorganic_Chemistry/Supplemental_Modules_and_Web_sites_(Inorganic_Chemistry)/Crystal_Field_Theory/Crystal_Field_Theory)

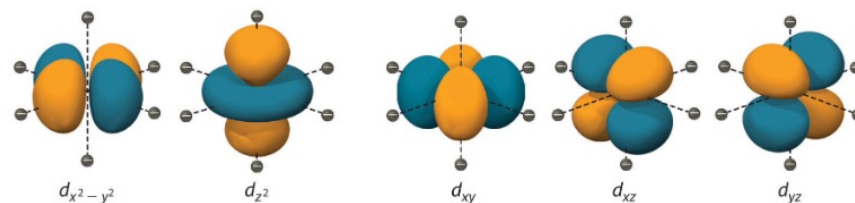


Figure 3: Spatial arrangement of ligands in an octahedral ligand field with respect to the five d-orbitals.

Square Planar Complexes

In a square planar, there are four ligands as well. However, the difference is that the electrons of the ligands are only attracted to the xy plane. Any orbital in the xy plane has a higher energy level (Figure 6). There are four different energy levels for the square planar (from the highest energy level to the lowest energy level): $d_{x^2-y^2}$, d_{xy} , d_{z^2} , and both d_{xz} and d_{yz} .

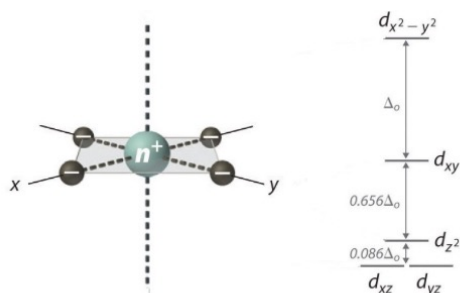


Figure 6: Splitting of the degenerate d-orbitals (without a ligand field) due to a square planar ligand field.

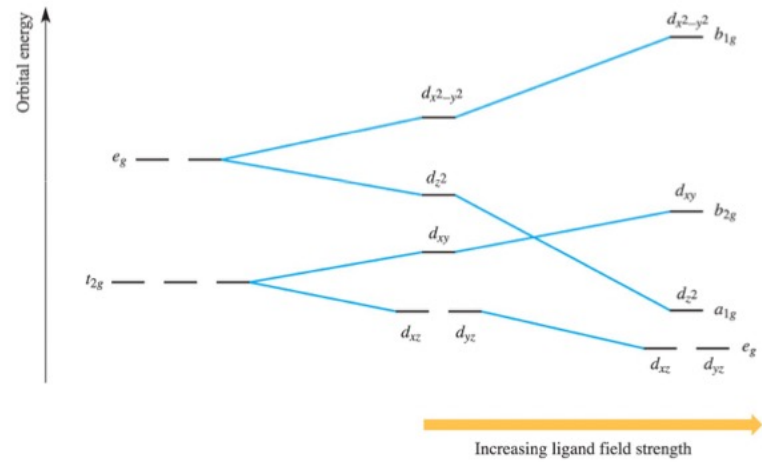
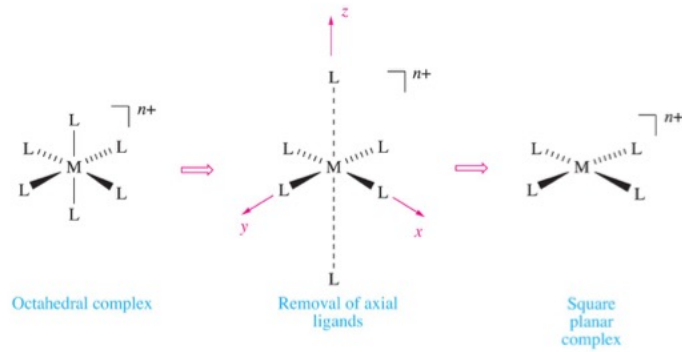
The splitting energy (from highest orbital to lowest orbital) is Δ_{sp} and tends to be larger than Δ_o .

$$\Delta_{sp} = 1.74 \Delta_o \quad (3)$$

Moreover, Δ_{sp} is also larger than the pairing energy, so the square planar complexes are usually **low spin** complexes.

Depending on the crystallographic environment the d-orbital energies split

Square Planar



Depending on the crystallographic environment the d-orbital energies split This impacts the Enthalpy of Formation

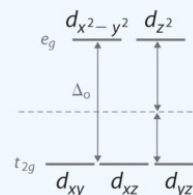
[https://chem.libretexts.org/Bookshelves/Inorganic_Chemistry/Supplemental_Modules_and_Web_sites_\(Inorganic_Chemistry\)/Crystal_Field_Theory/Crystal_Field_Theory](https://chem.libretexts.org/Bookshelves/Inorganic_Chemistry/Supplemental_Modules_and_Web_sites_(Inorganic_Chemistry)/Crystal_Field_Theory/Crystal_Field_Theory)

Blocks in the periodic table

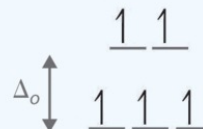
For the complex ion $[\text{Fe}(\text{Cl})_6]^{3-}$ determine the number of d electrons for Fe, sketch the d-orbital energy levels and the distribution of d electrons among them, list the number of lone electrons, and label whether the complex is paramagnetic or diamagnetic.

Solution

- Step 1: Determine the oxidation state of Fe. Here it is Fe^{3+} . Based on its electron configuration, Fe^{3+} has **5 d-electrons**.
- Step 2: Determine the geometry of the ion. Here it is an octahedral which means the energy splitting should look like:



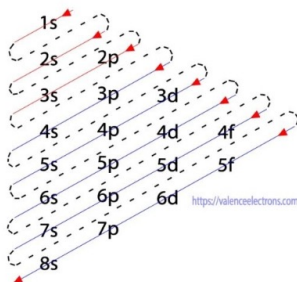
- Step 3: Determine whether the ligand induces a strong or weak field spin by looking at the **spectrochemical series**. Cl^- is a weak field ligand (i.e., it induces high spin complexes). Therefore, electrons fill all orbitals before being paired.



- Step four: Count the number of lone electrons. Here, there are **5 electrons**.
- Step five: The five unpaired electrons means this complex ion is **paramagnetic** (and strongly so).

Electron Configuration in the Aufbau principle

$$\begin{aligned} s &= 2 \\ p &= 6 \\ d &= 10 \\ f &= 14 \end{aligned}$$



$$26 - 3 = 23 = 2 + 2 + 6 + 2 + 6 + (5 \text{ d}). \text{ Unpaired electrons } \Rightarrow \text{Paramagnetic}$$

Depending on the crystallographic environment the d-orbital energies split This impacts the Enthalpy of Formation

[https://chem.libretexts.org/Bookshelves/Inorganic_Chemistry/Supplemental_Modules_and_Web_sites_\(Inorganic_Chemistry\)/Crystal_Field_Theory/Crystal_Field_Theory](https://chem.libretexts.org/Bookshelves/Inorganic_Chemistry/Supplemental_Modules_and_Web_sites_(Inorganic_Chemistry)/Crystal_Field_Theory/Crystal_Field_Theory)

A *tetrahedral* complex absorbs at 545 nm. What is the respective octahedral crystal field splitting (Δ_o)? What is the color of the complex?

Solution

$$\begin{aligned}\Delta_t &= \frac{hc}{\lambda} \\ &= \frac{(6.626 \times 10^{-34} \text{ J} \cdot \text{s})(3 \times 10^8 \text{ m/s})}{545 \times 10^{-9} \text{ m}} \\ &= 3.65 \times 10^{-19} \text{ J}\end{aligned}$$

However, the *tetrahedral* splitting (Δ_t) is $\sim 4/9$ that of the *octahedral* splitting (Δ_o).

$$\begin{aligned}\Delta_t &= 0.44\Delta_o \\ \Delta_o &= \frac{\Delta_t}{0.44} \\ &= \frac{3.65 \times 10^{-19} \text{ J}}{0.44} \\ &= 8.30 \times 10^{-18} \text{ J}\end{aligned}$$

This is the energy needed to promote *one* electron in *one* complex. Often the crystal field splitting is given per mole, which requires this number to be multiplied by Avogadro's Number (6.022×10^{23}).

This complex appears red, since it absorbs in the complementary green color (determined via the color wheel).

Depending on the crystallographic environment the d-orbital energies split
 This impacts the Enthalpy of Formation

Crystal Field Effect

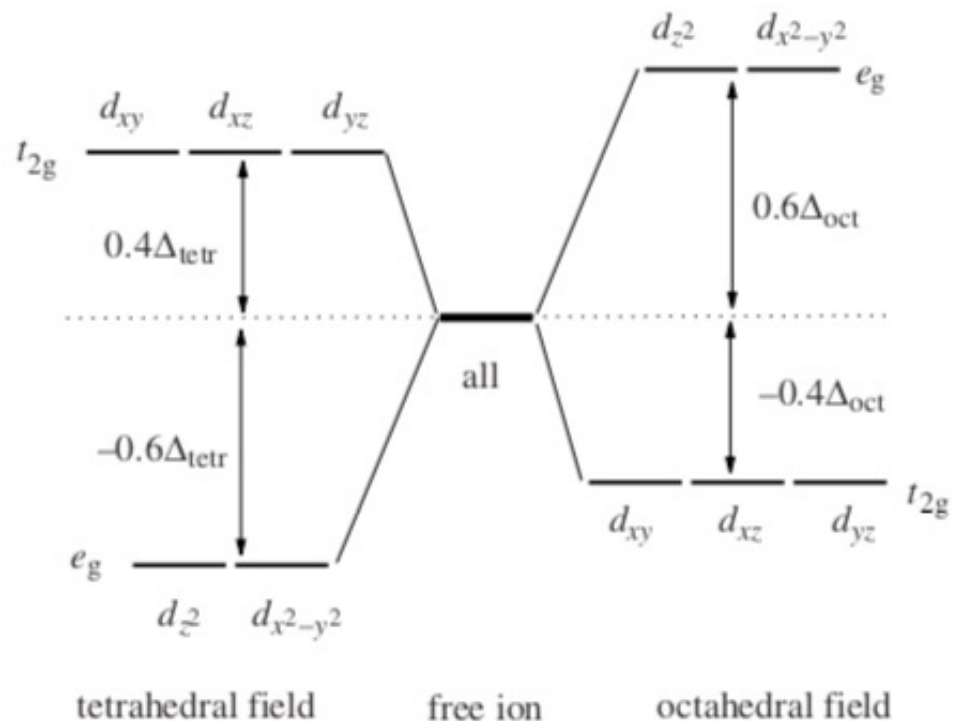


Figure 7.8 d level splitting for octahedral and tetrahedral crystal fields.

Crystal Field Stabilization Energy

Factors affecting the CFSE

First, note that the pairing energies for first-row transition metals are relatively constant.

Therefore, the difference between strong- and weak-field, or low and high- spin cases comes down to the magnitude of the crystal field splitting energy (Δ).

1. Geometry is one factor, Δ_o is larger than Δ_t

In almost all cases, the Δ_t is smaller than P (pairing energy), so...

Tetrahedral complexes are always weak-field (high spin)

Square planar complexes may either be weak- or strong-field.

2. Oxidation State of Metal Cation –

A greater charge on cation results in a greater magnitude of Δ

Why? A greater charge pulls ligands more strongly towards the metal, therefore influences the splitting of the energy levels more.

3. Size of the Metal Cation –

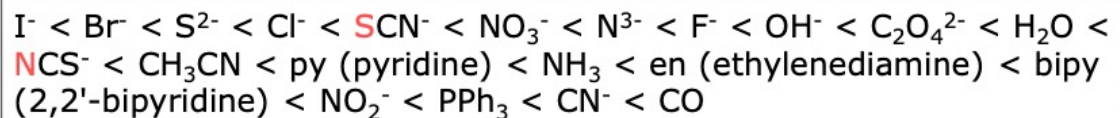
For second and third-row transition metal ions, Δ_o is larger than first-row.

Less steric hindrance between the ligands – better overlap w/orbitals.

Crystal Field Stabilization Energy

4. Identity of the ligands.

A spectrochemical series has been developed and sorted by the ability to split metal d-orbitals.



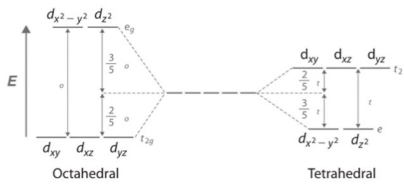
As the ligands decrease in size, their ability to split the d-orbitals increases. The larger and bulkier ligands exhibit more steric hindrance and approach the metal less effectively.

One might expect that ligands with a negative charge might split the d-orbitals better, but this is not always the case. Notice that water is higher in the series than OH^- , even though O on OH^- has a high concentration of charge.

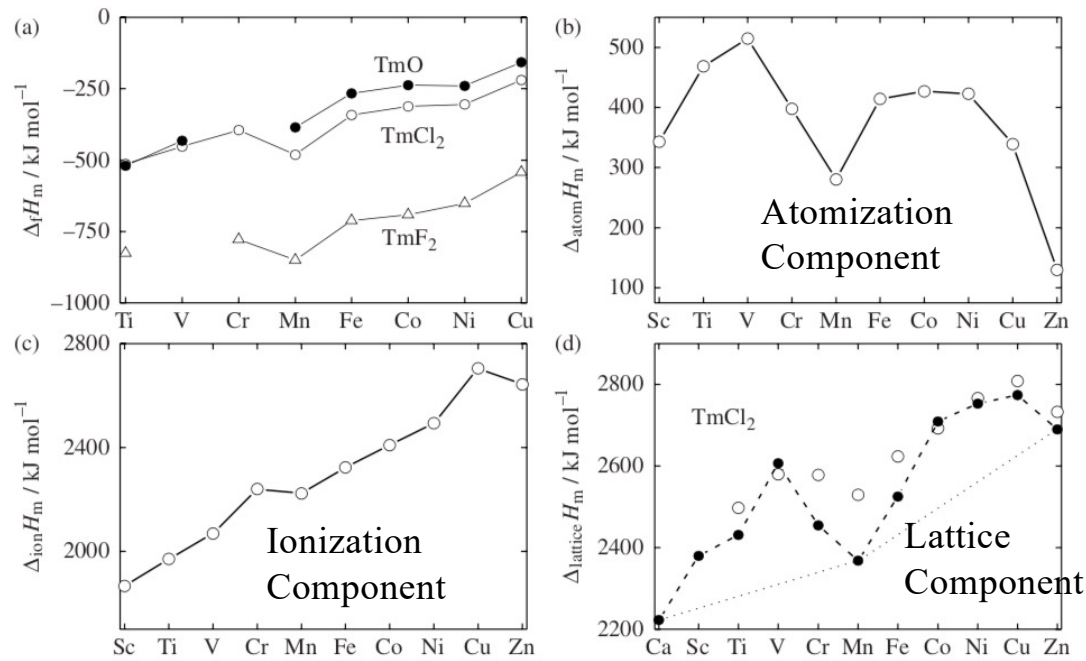
The dipole moment of H_2O is larger than NH_3 , but NH_3 is higher in the series. PPh_3 is high in the series, but also very bulky, neutral and has a small dipole moment.

Transition metal lattice stabilization due to d-orbital splitting

First series chlorides, oxides and fluorides
Increasing d electrons



$$\Delta_f H_m(MX) = -\Delta_{latt} H_m + \Delta_{atom} H_m + \Delta_{ion} H_m + \Delta_{diss} H_m + \Delta_{eg} H_m$$



Crystal Field Stabilization due to d-orbital splitting (not for Ca, Mn, Zn)

Figure 7.9 Thermodynamic data (b)–(d) needed in analysis of the enthalpy of formation of the binary transition metal compounds given in (a). (b) Atomization enthalpy of first series transition metals; (c) sum of first and second ionization enthalpies of first series transition metals; (d) derived lattice enthalpy of transition metal dihalides.

Increasing electronegativity

H 2.1																	F 4.0
																	Cl 3.0
																	Br 2.8
																	I 2.5
V 1.6	Cr 1.6	Mn 1.5	Fe 1.8	Co 1.9	Ni 1.9	Cu 1.9	Zn 1.6	Ga 1.6	Ge 1.8	As 2.0	Se 2.4	Br 2.8	I 2.5	At 2.2			
Nb 1.6	Mo 1.8	Tc 1.9	Ru 2.2	Rh 2.2	Pd 2.2	Ag 1.9	Cd 1.7	In 1.7	Sn 1.8	Sb 1.9	Te 2.1						
Ta 1.5	W 1.7	Re 1.9	Os 2.2	Ir 2.2	Pt 2.2	Au 2.4	Hg 1.9	Tl 1.8	Pb 1.9	Bi 1.9	Po 2.0						
Pa 1.4	U 1.4	Np-No 1.4-1.3															

Heat of Formation for Transition Metal Oxides in Different Oxidation States

Basic (at low oxidation state)	Transition Metals										oxidation state
21 Sc	22 Ti	23 V	24 Cr	25 Mn	26 Fe	27 Co	28 Ni	29 Cu	30 Zn		
39 Y	40 Zr	41 Nb	42 Mo	43 Tc	44 Ru	45 Rh	46 Pd	47 Ag	48 Cd		
57 La	72 Hf	73 Ta	74 W	75 Re	76 Os	77 Ir	78 Pt	79 Au	80 Hg		
89 Ac	104 Rf	105 Db	106 Sg	107 Bh	108 Hs	109 Mt	110 Ds	111 Rg	112 Cn		

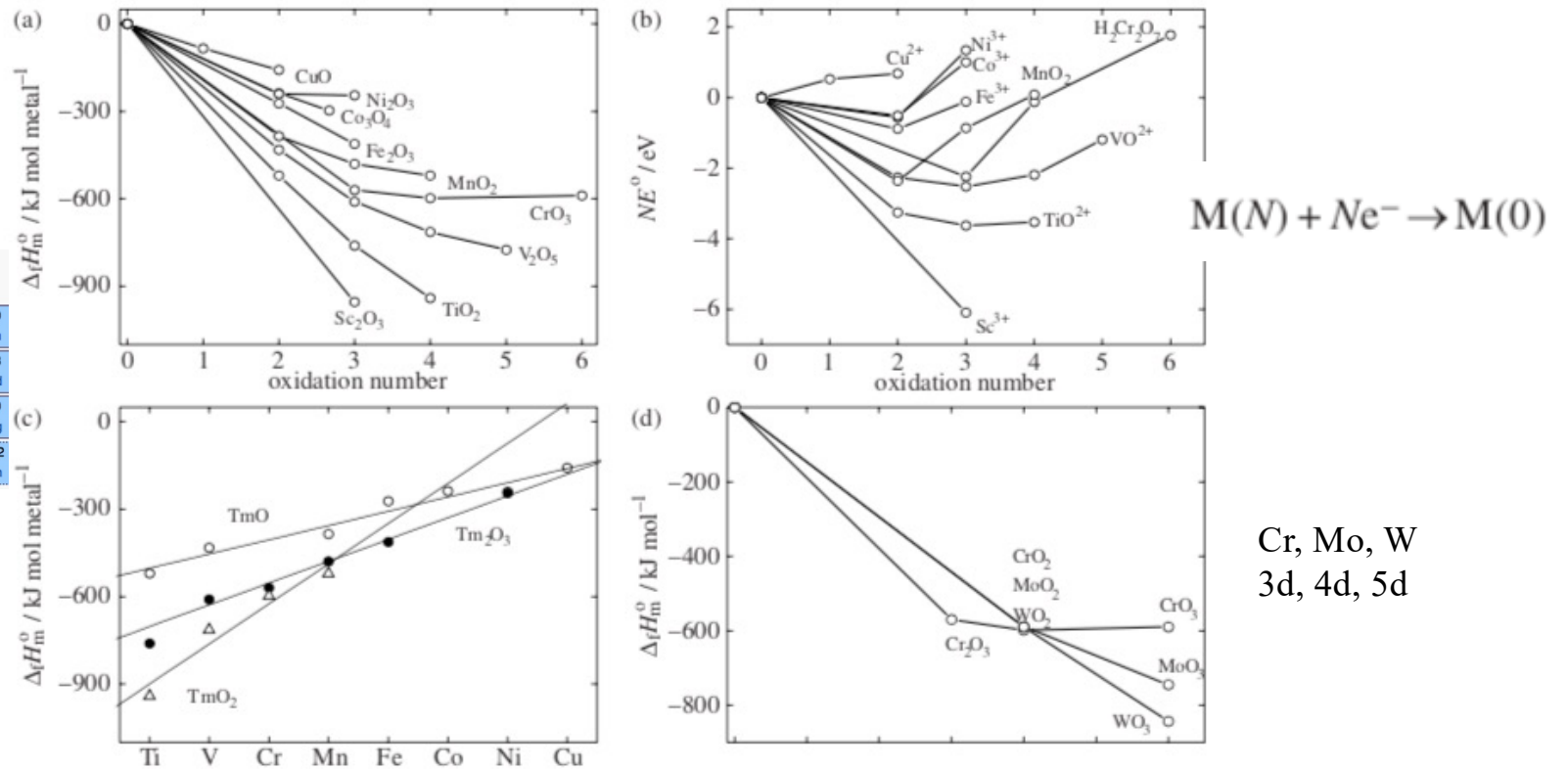
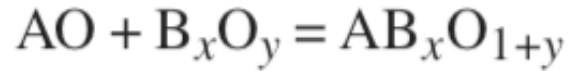


Figure 7.11 Enthalpy of formation of binary oxides of the 3d transition metals (a) and (c), Frost diagram for the same 3d metals (b) Enthalpy of formation of binary oxides of the group 6 transition metals.

Cr, Mo, W
3d, 4d, 5d

Acid-Base Model for Heat of Formation of Ternary Oxides



Basicity
 $MgO < CaO < SrO < BaO$

Na_2O
 Base
 transfers
 its oxygen
 s-block
 oxides

SiO_2
 Acid
 accepts
 oxygen
 p-block
 oxides
 SiO_4^{2-}

$SiNa_2O_3$
 Acidity
 $Al < Si < P < S$

Blocks in the periodic table [hide]

Group	1	2	3	4	5	6	7	8	9	10	11	12	13	14	15	16	17	18		
1	1 H																	2 He		
2	3 Li	4 Be											5 B	6 C	7 N	8 O	9 F	10 Ne		
3	11 Na	12 Mg											13 Al	14 Si	15 P	16 S	17 Cl	18 Ar		
4	19 K	20 Ca	21 Sc			22 Ti	23 V	24 Cr	25 Mn	26 Fe	27 Co	28 Ni	29 Cu	30 Zn	31 Ga	32 Ge	33 As	34 Se	35 Br	36 Kr
5	37 Rb	38 Sr	39 Y			40 Zr	41 Nb	42 Mo	43 Tc	44 Ru	45 Rh	46 Pd	47 Ag	48 Cd	49 In	50 Sn	51 Sb	52 Te	53 I	54 Xe
6	55 Cs	56 Ba	57 La	*		72 Hf	73 Ta	74 W	75 Re	76 Os	77 Ir	78 Pt	79 Au	80 Hg	81 Tl	82 Pb	83 Bi	84 Po	85 At	86 Rn
7	87 Fr	88 Ra	89 Ac	**		104 Rf	105 Db	106 Sg	107 Bh	108 Hs	109 Mt	110 Ds	111 Rg	112 Cn	113 Nh	114 Fl	115 Mc	116 Lv	117 Ts	118 Og
						58 Ce	59 Pr	60 Nd	61 Pm	62 Sm	63 Eu	64 Gd	65 Tb	66 Dy	67 Ho	68 Er	69 Tm	70 Yb	71 Lu	
						90 Th	91 Pa	92 U	93 Np	94 Pu	95 Am	96 Cm	97 Bk	98 Cf	99 Es	100 Fm	101 Md	102 No	103 Lr	

s-block p-block d-block f-block Background color shows the block of the periodic table
Primordial From decay Synthetic Border shows natural occurrence of the element

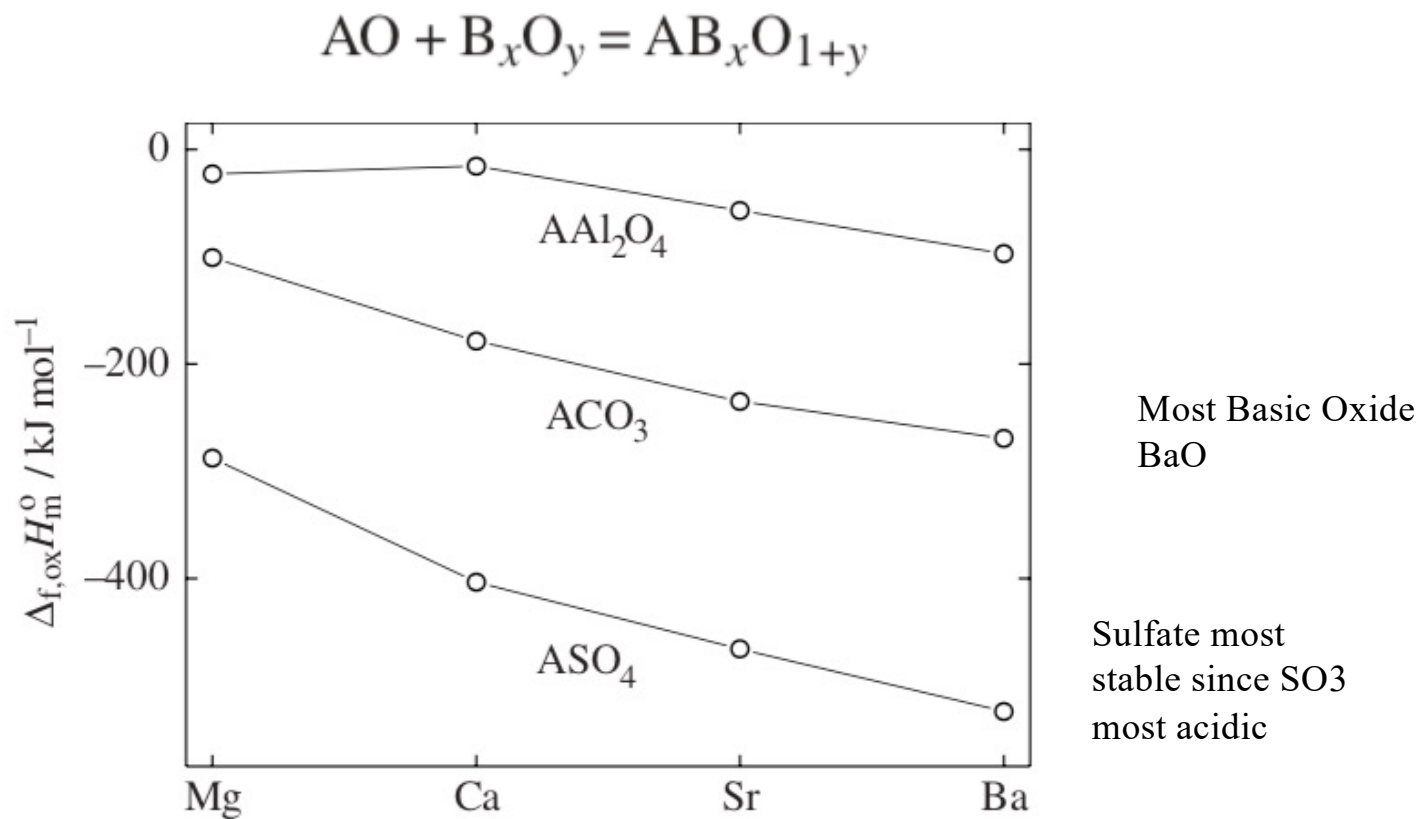


Figure 7.14 Enthalpy of formation of selected ternary oxides from their binary constituents.

Ionic potential
 $e^-/\text{ionic radius } (\text{\AA})$
 q/r
 <2 strong base
 2-4 basic
 4-7 amphoteric
 >7 acidic

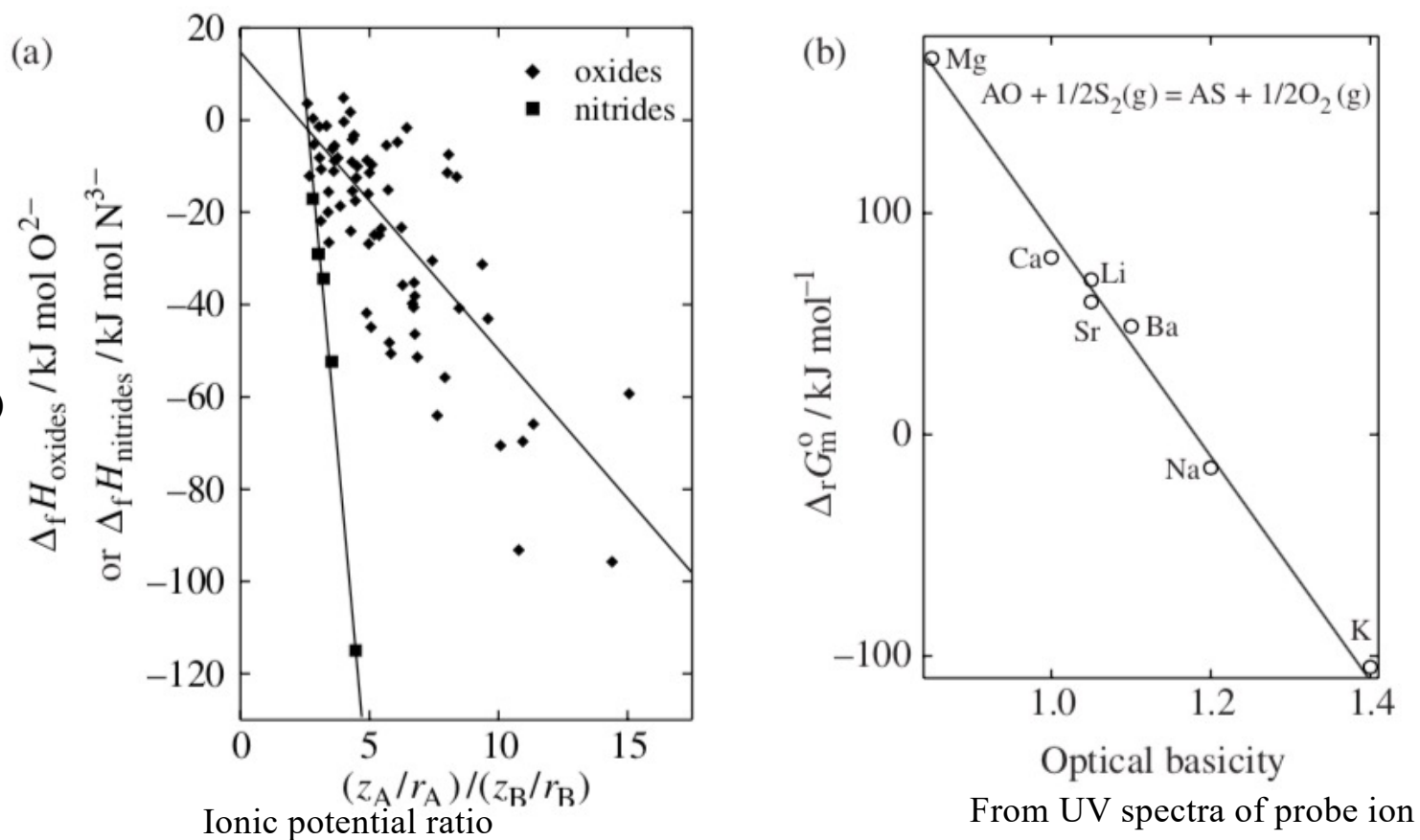


Figure 7.15 (a) Enthalpy of formation of ternary oxides and nitrides from their binary constituent compounds as a function of the ratio of ionic potential [16]. Reprinted with permission from [16] Copyright (1997) American Chemical Society. (b) Gibbs energy of the oxide–sulfide equilibrium for group 1 and 2 metals at 1773 K as a function of the optical basicity of the metal.

Atomic Size

Perovskite structure

Calcium titanate CaTiO_3

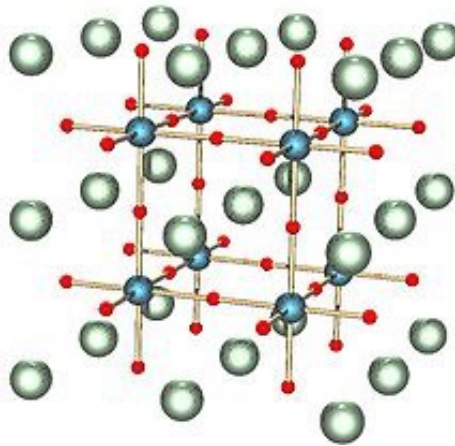
Embed cations in the structure for engineered properties

One is solar energy absorption in Graetzel cells

These are the most promising low-temperature formation PV devices

(silicon solar cells require high temperature reduction of silica and chemical purification)

Red O^{2-}
Blue Ti^{4+}
Green Ca^{2+} or Ba^{2+}



Cubic/Orthorhombic-like structure

Can accommodate many transition metals

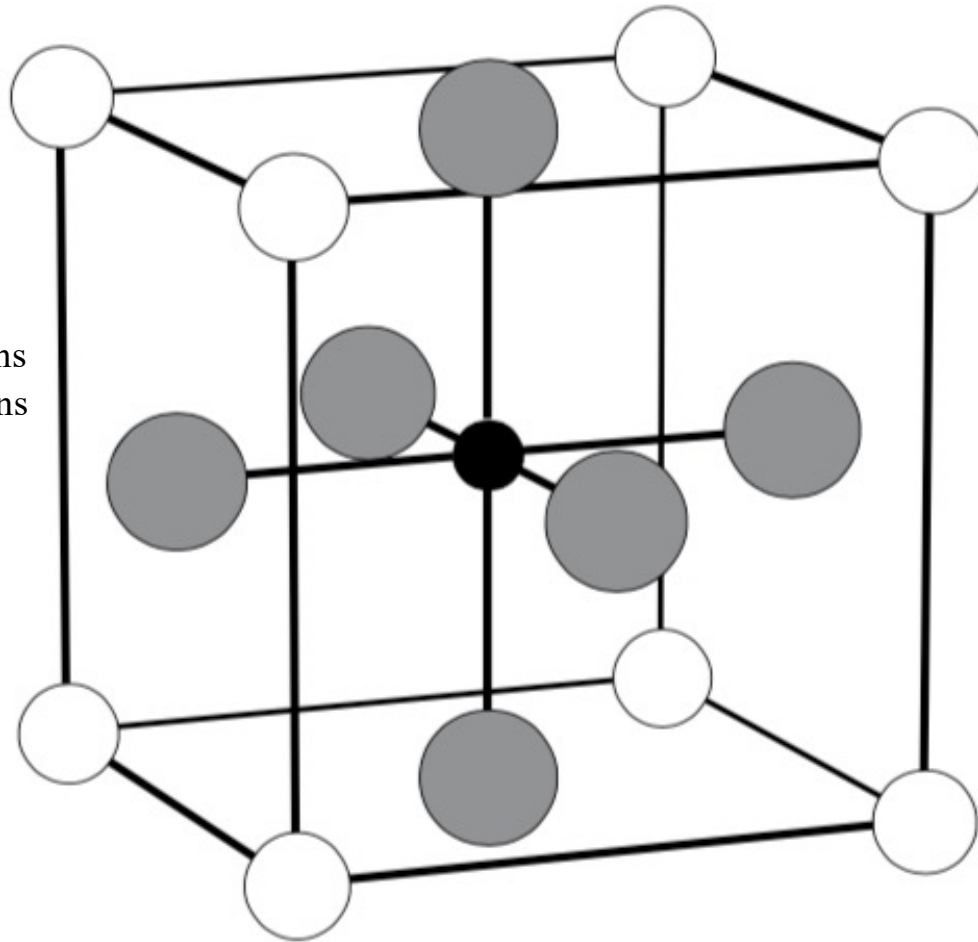
ABX_3

A is much larger than B cations, X is anion (oxide)

B has 6-fold coordination surrounded by octahedron of anions

A has 12-fold cubahedral coordination

A is simple cubic
With O in the face center positions
And B in the body center positions



$$t = \frac{r_{AO}}{\sqrt{2}r_{BO}} = \frac{r_A + r_O}{\sqrt{2}(r_B + r_O)}$$

$t = 1$ Perfect Cubic
 $0.8 < t < 1.1$

Figure 7.16 The perovskite-type structure. Small black circles represent the B atom, large grey circles represent O atoms and open circles represent the A atom.

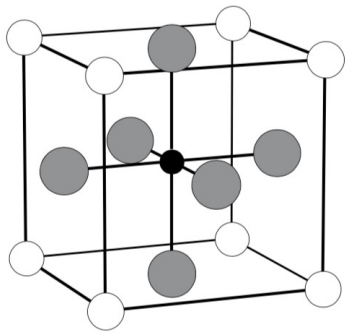


Figure 7.16 The perovskite-type structure. Small black circles represent the B atom, large grey circles represent O atoms and open circles represent the A atom.

$$t = \frac{r_{AO}}{\sqrt{2}r_{BO}} = \frac{r_A + r_O}{\sqrt{2}(r_B + r_O)}$$

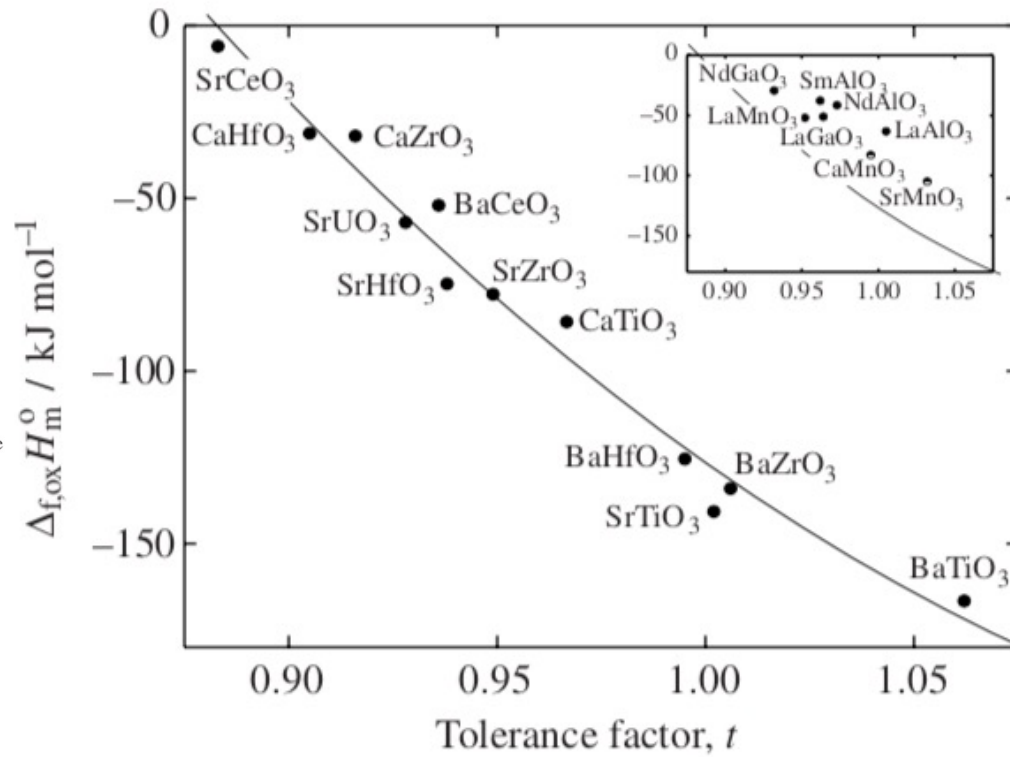
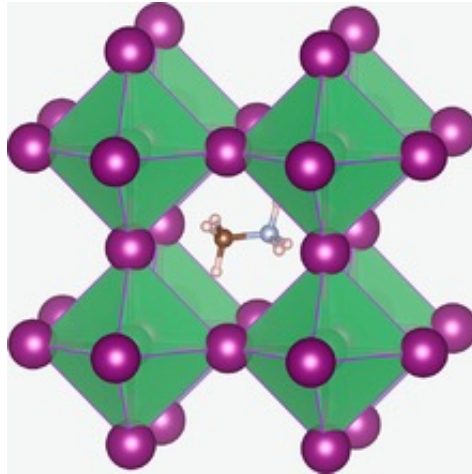


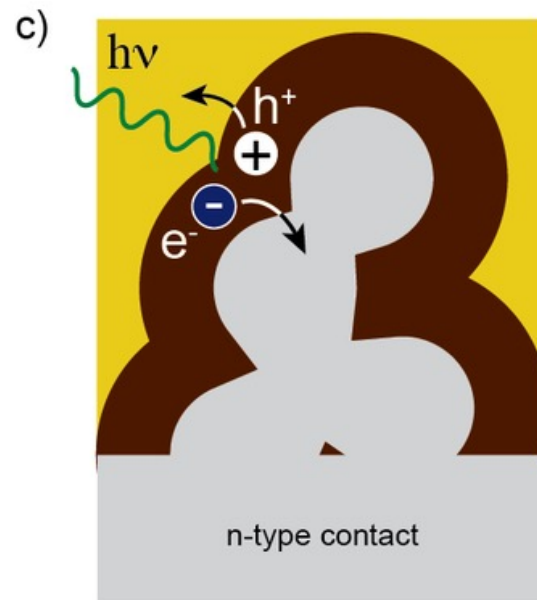
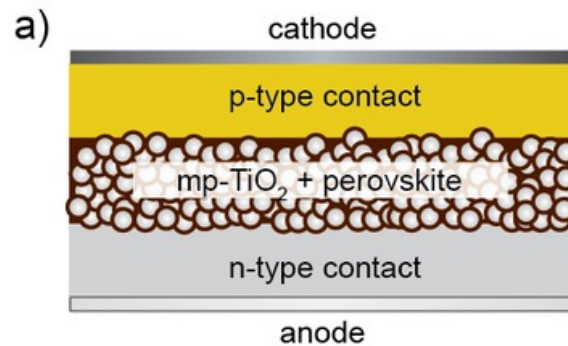
Figure 7.17 Enthalpy of formation of selected perovskite-type oxides as a function of the tolerance factor. Main figure show data for perovskites where the A atom is a Group 2 element and B is a d or f element that readily takes a tetravalent state [19, 20]. The insert shows enthalpies of formation of perovskite-type oxides where the A atom is a trivalent lanthanide metal [21] or a divalent alkaline earth metal [22] whereas the B atom is a late transition metal atom or Ga/Al.

Methyl Ammonium Lead Halide

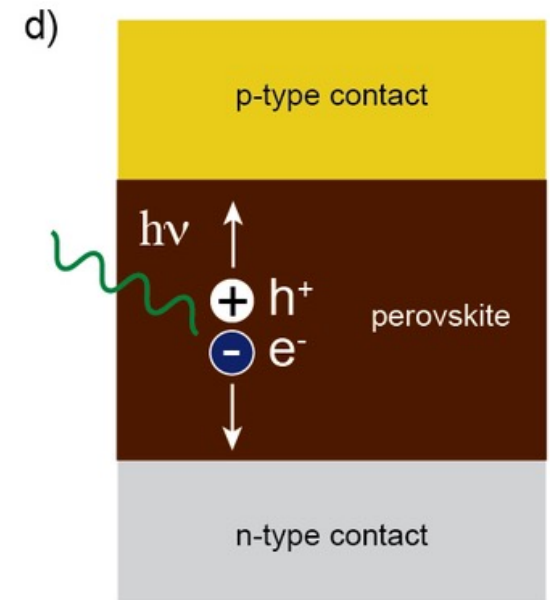
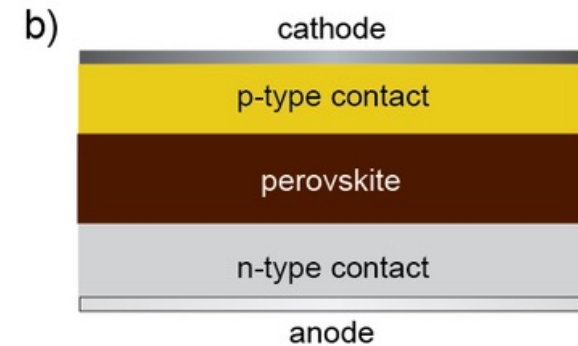


Schematic of a sensitized perovskite solar cell in which the active layer consists of a layer of [mesoporous TiO₂](#) which is coated with the perovskite absorber. The active layer is contacted with an n-type material for electron extraction and a p-type material for hole extraction. b) Schematic of a [thin-film](#) perovskite solar cell. In this architecture in which just a flat layer of perovskite is sandwiched between two selective contacts. c) Charge generation and extraction in the sensitized architecture. After light absorption in the perovskite absorber the photogenerated electron is injected into the mesoporous TiO₂ through which it is extracted. The concomitantly generated hole is transferred to the p-type material. d) Charge generation and extraction in the thin-film architecture. After light absorption both charge generation as well as charge extraction occurs in the perovskite layer.

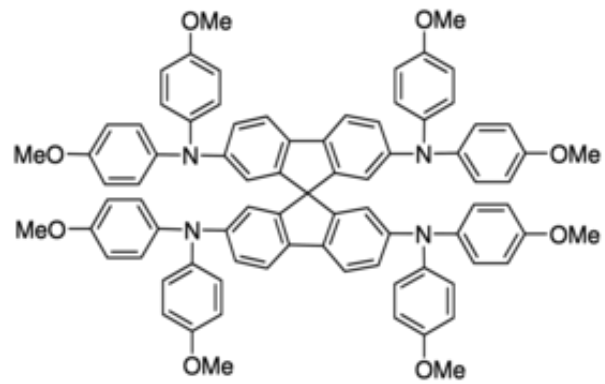
Sensitized perovskite solar cell



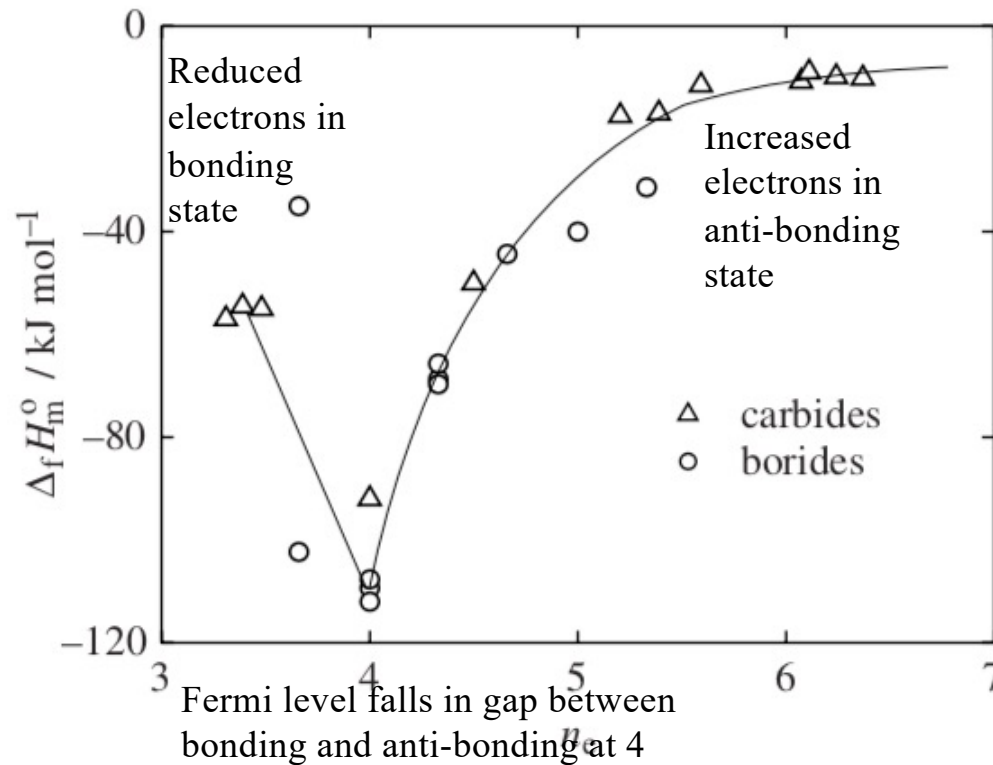
Thin-film perovskite solar cell



spiro Ometad p-type semi-conductor



Enthalpy of Formation versus Number of Valence Electrons



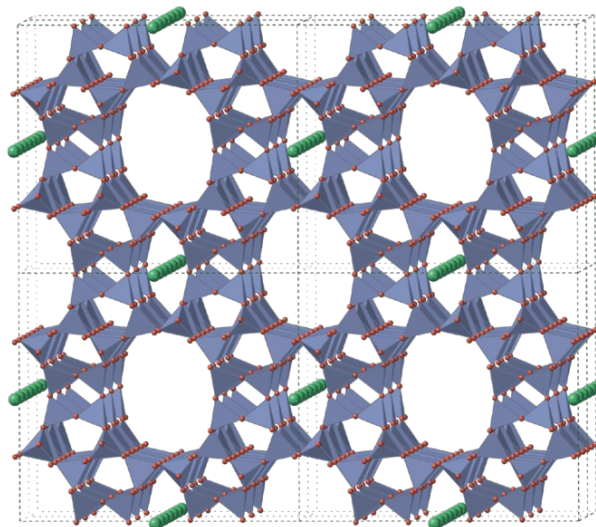
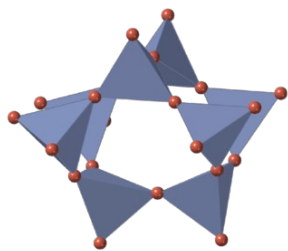
TiC with $n_e = 4$ has a high enthalpy of formation since the Fermi level falls in a pronounced gap in density of electronic states separating bonding and anti-bonding electron bands.

Figure 7.18 Enthalpy of formation of binary carbides and diborides [25, 26] as a function of the average number of valence electrons per atom.

Zeolites (Natural are aluminosilicate rocks, synthetic can be a variety of materials often based on SiO_2)



secondary building unit (cage)



Mordenite (MOR framework)



Microscopic structure of a zeolite ([mordenite](#)) framework, assembled from tetrahedra. Sodium is present as an extra-framework cation (in green).

Can form meso or micro pores (colloidal- or nano-scale) (These are terms from gas adsorption field.)

Reference 29

Synthetic Zeolites can have meso (colloidal) or micro (nano) pores depending on the templating material and synthesis conditions. Usually start with TEOS and a surfactant or block copolymer

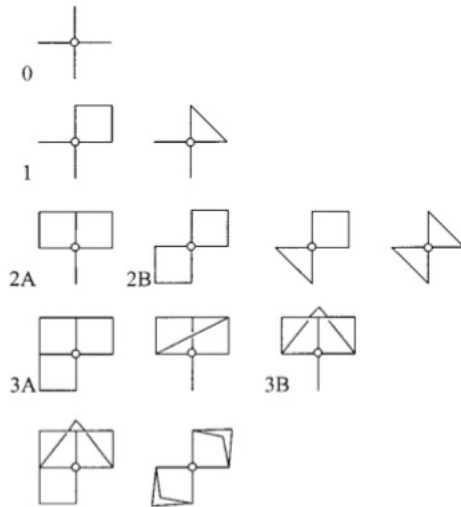


Figure 5. Configuration loops present in zeolites.

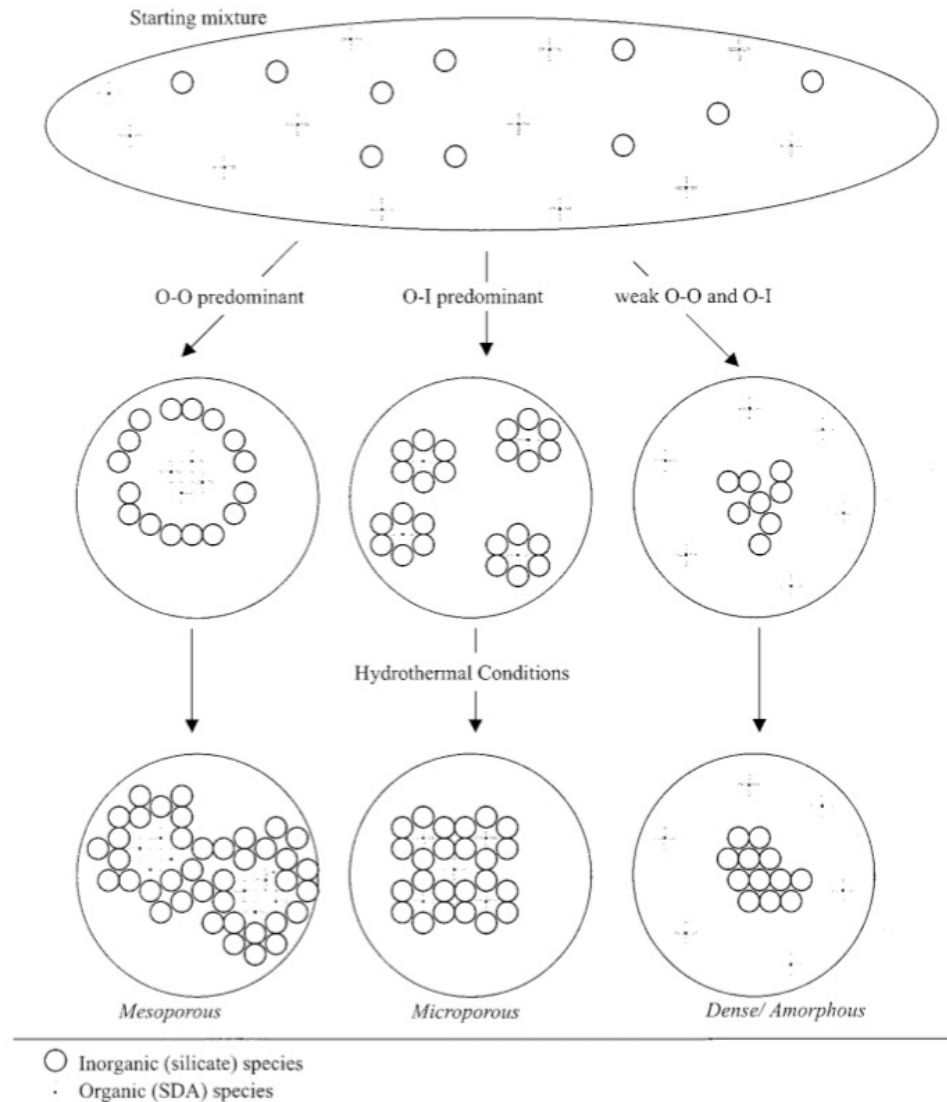


Figure 1. Possibilities for silicate self-assembly in hydrothermal syntheses.

Surface effect as we saw earlier except that this is on a molecular/nano scale

Enthalpy relative to quartz

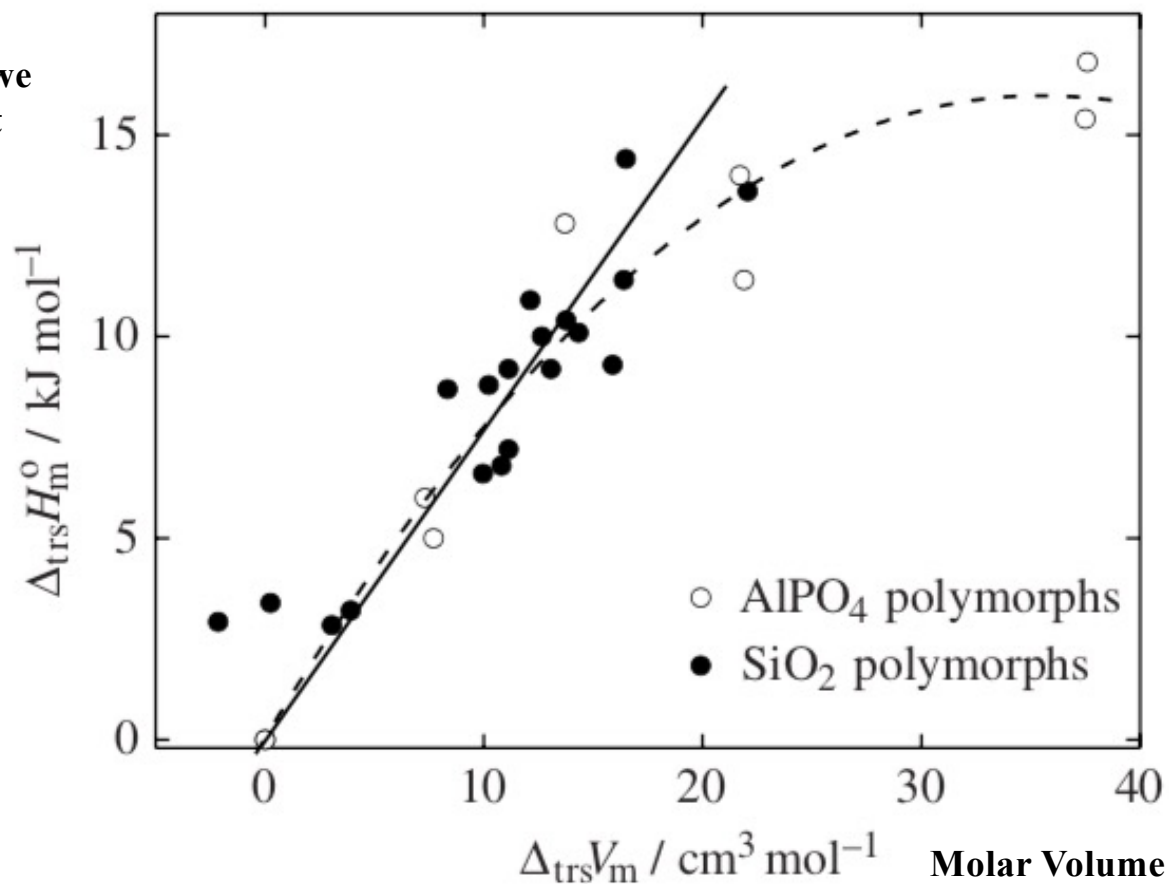


Figure 7.19 Enthalpy of transition from the stable polymorph versus volume correlations for micro- and mesoporous SiO_2 and AlPO_4 materials [29, 34].

Energy of Formation for Substitutional Solid Solutions

Atomic Radii => Volume of compounds

Hume-Rothery Rule limited solubility if size difference exceeds 15%

Electronegativity

Large difference in binary system leads to negative enthalpy of mixing Pd-Zr and is small for systems with low or no electronegativity and size difference Ti-Zr

Valence electron density

Binary components have the same crystal structure

Large enthalpy of mixing is related to large number of intermetallic phases

Elastic contribution to the enthalpy of mixing, small mixes well with large

$$\Delta_{\text{mix}} H_m = x_A x_B^2 c_A \frac{\Delta V^2}{3V_A} + x_B x_A^2 c_B \frac{\Delta V^2}{3V_B}$$

c_i are constants x_i mole fractions V molar volumes
Sub-regular solution model

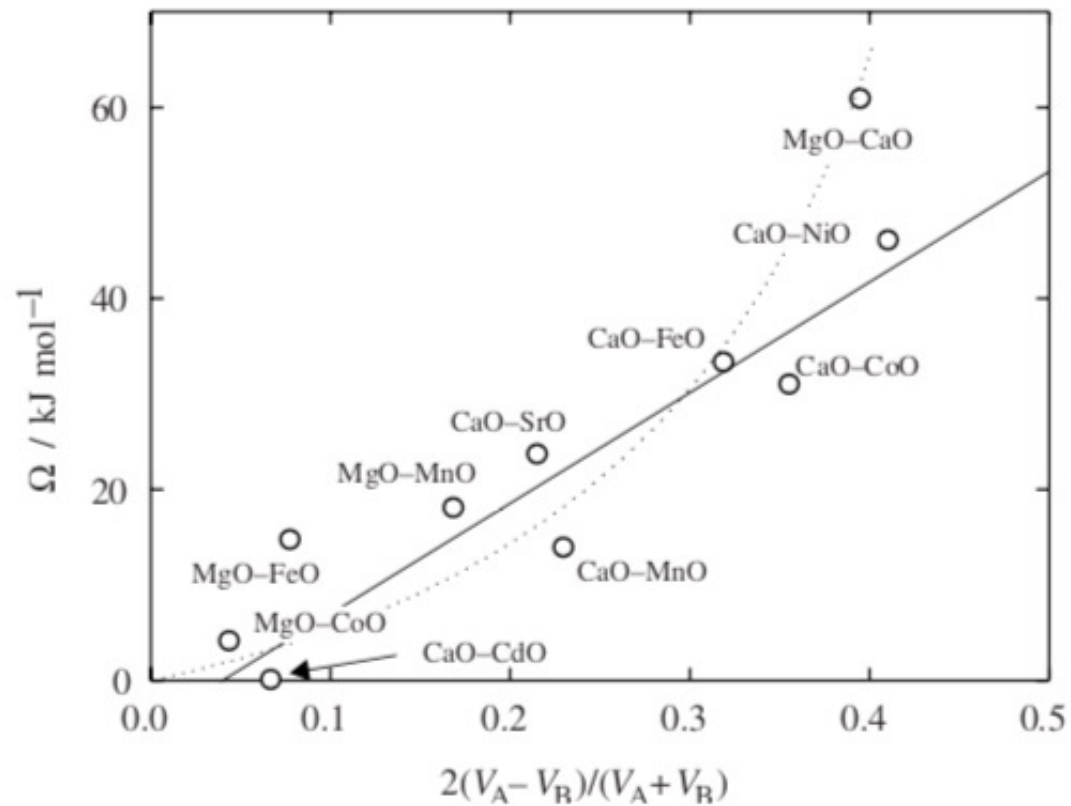


Figure 7.21 Enthalpies of mixing of selected NaCl-type systems involving the alkali earth oxides. The solid and dashed lines show scaling with the volume mismatch and with the square of the volume mismatch, respectively.

Energy of Formation for Interstitial Solid Solutions

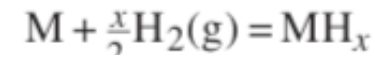
Elastic interactions

Electronic interactions

Gas solubility in metals

Temperature

Pressure solubility for H_2 $x \sim \sqrt{p}$



$$x \propto \sqrt{\frac{P}{P_0}} \exp\left(\frac{\Delta_{7.22} S}{R}\right) \exp\left(\frac{\Delta_{7.22} H}{RT}\right)$$

Sievert's Law

Solubility of gasses in metals

Blocks in the periodic table [hide]

3	4	5	6	7	8	9	10	11	12	13	14	15	16	17	18
															2 He
										5 B	6 C	7 N	8 O	9 F	10 Ne
										13 Al	14 Si	15 P	16 S	17 Cl	18 Ar
21 Sc	22 Ti	23 V	24 Cr	25 Mn	26 Fe	27 Co	28 Ni	29 Cu	30 Zn	31 Ga	32 Ge	33 As	34 Se	35 Br	36 Kr
39 Y	40 Zr	41 Nb	42 Mo	43 Tc	44 Ru	45 Rh	46 Pd	47 Ag	48 Cd	49 In	50 Sn	51 Sb	52 Te	53 I	54 Xe
57 La	* 72 Hf	73 Ta	74 W	75 Re	76 Os	77 Ir	78 Pt	79 Au	80 Hg	81 Tl	82 Pb	83 Bi	84 Po	85 At	86 Rn
89 Ac	* 104 Rf	105 Db	106 Sg	107 Bh	108 Hs	109 Mt	110 Ds	111 Rg	112 Cn	113 Nh	114 Fl	115 Mc	116 Lv	117 Ts	118 Og
		* 58 Ce	59 Pr	60 Nd	61 Pm	62 Sm	63 Eu	64 Gd	65 Tb	66 Dy	67 Ho	68 Er	69 Tm	70 Yb	71 Lu
		** 90 Th	91 Pa	92 U	93 Np	94 Pu	95 Am	96 Cm	97 Bk	98 Cf	99 Es	100 Fm	101 Md	102 No	103 Lr

s-block f-block Background color shows the block of the periodic table
 Primordial From decay Synthetic Border shows natural occurrence of the element

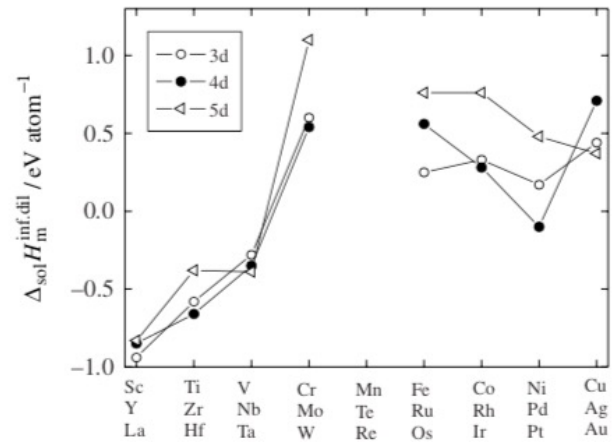


Figure 7.22 Enthalpy of solution of hydrogen in transition metals at infinite dilution [45].

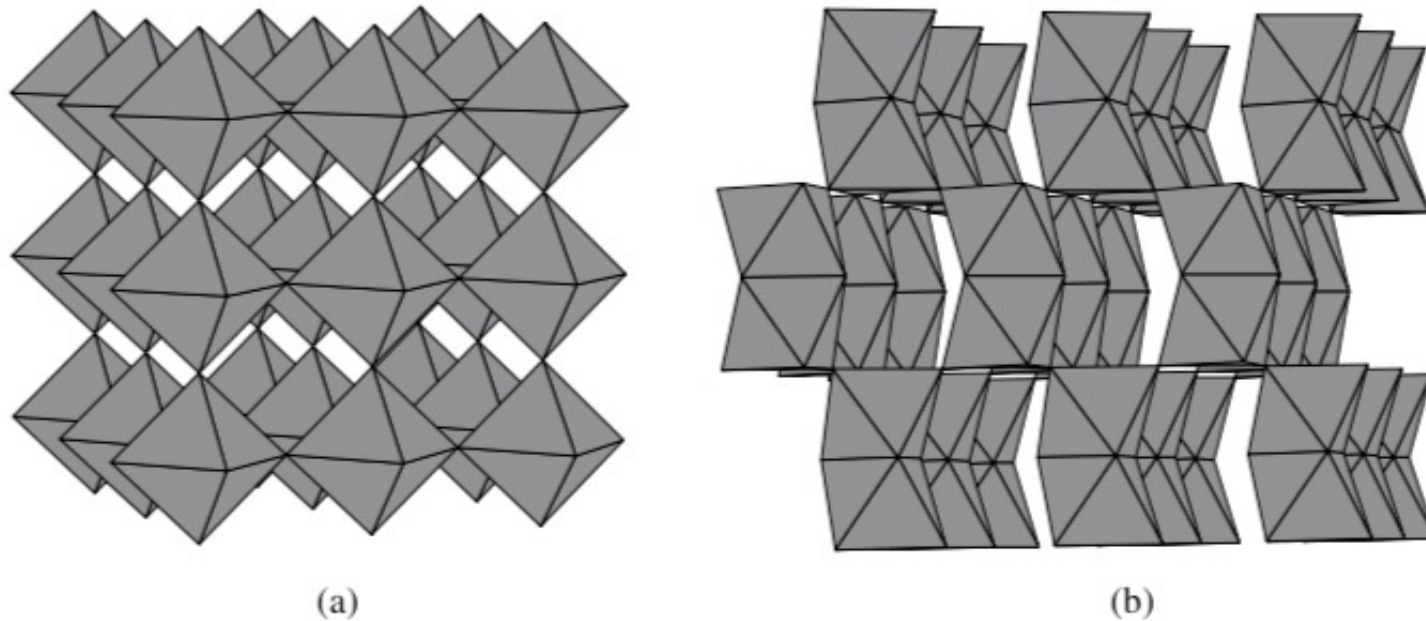


Figure 7.23 Connectivity of transition metal BO_6 octahedra in (a) cubic and (b) hexagonal perovskite SrMnO_3 .

6 kJ/mole difference in formation enthalpy
 Reduction temperature is 600K higher for hexagonal
 Cubic reduced $\text{SrMnO}_{2.5}$ is more stable
 Octahedral corners shared in cubic, faces shared in hexagonal
 High vacancies in faces make reduced hexagonal unfavorable

Liquid-Liquid Miscibility

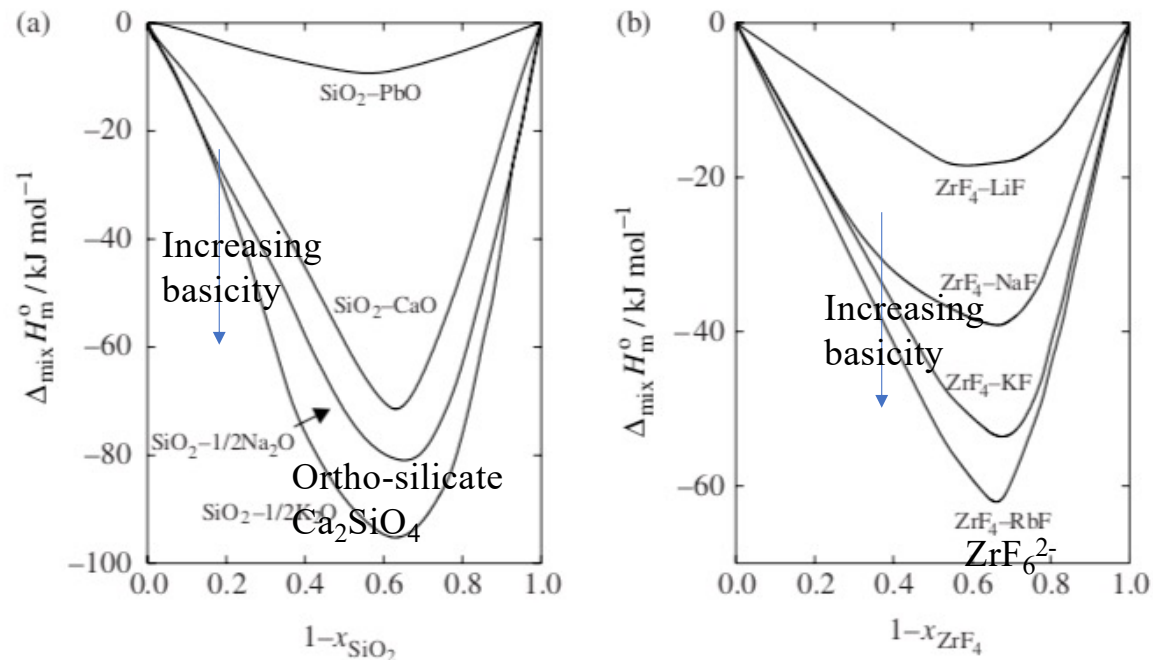
Mixing of acidic (SiO_2) and Basic (CaO) oxides Si^{4+} has coordination number 4 and Ca^{2+} has 6
 SiO_2 mixes well with CaO but CaO has a harder time mixing with SiO_2

ks in the periodic table [hide]

7	8	9	10	11	12	13	14	15	16	17	18
										2	He
						5	6	7	8	9	10
						B	C	N	O	F	Ne
						13	14	15	16	17	18
						Al	Si	P	S	Cl	Ar
25	26	27	28	29	30	31	32	33	34	35	36
Vn	Fe	Co	Ni	Cu	Zn	Ga	Ge	As	Se	Br	Kr
43	44	45	46	47	48	49	50	51	52	53	54
Tc	Ru	Rh	Pd	Ag	Cd	In	Sn	Sb	Te	I	Xe
75	76	77	78	79	80	81	82	83	84	85	86
Re	Os	Ir	Pt	Au	Hg	Tl	Pb	Bi	Po	At	Rn
07	108	109	110	111	112	113	114	115	116	117	118
Bh	Hs	Mt	Ds	Rg	Cn	Nh	Fl	Mc	Lv	Ts	Og
61	62	63	64	65	66	67	68	69	70	71	
Pm	Sm	Eu	Gd	Tb	Dy	Ho	Er	Tm	Yb	Lu	
93	94	95	96	97	98	99	100	101	102	103	
Np	Pu	Am	Cm	Bk	Cf	Es	Fm	Md	No	Lr	

shows the block of the periodic table

Synthetic Border shows natural occurrence of the element



ZrF_4 strong acid

Figure 7.24 Enthalpy of mixing of (a) binary silicate [48] (reprinted by permission of A. Navrotsky) and (b) fluoride systems [49].

Liquid Salt Mixtures

Size parameter, $d = (d_A - d_B)/(d_A + d_B)$

Common Anions mix with negative enthalpy of mixing
Common cations do not mix due to anion-anion repulsion

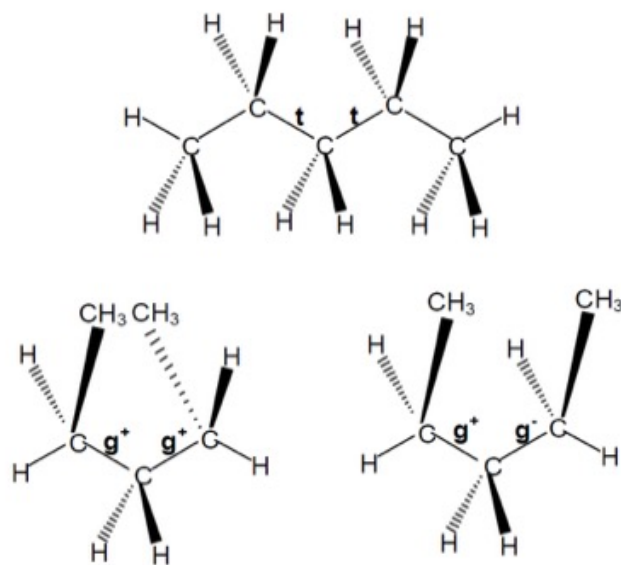
Conformational Enthalpy of Polymers

The Rotational Isomeric State Model of Volkenstein and Paul Flory (Nobel Prize)

Carbon has a tetrahedral bonding arrangement

For a chain of carbon, the two side groups interact with the side groups of neighboring carbons

For Butene



“Trans” is sterically the most favorable arrangement

“Gauche +” and “Gauche -” are less favorable

The Boltzmann equation gives the probability of a particular conformation, **Z is the partition function** or the sum of all the different Boltzmann expressions in an ensemble

$$P(\varphi_i) = \frac{\exp(-E(\varphi_i)/kT)}{Z}$$

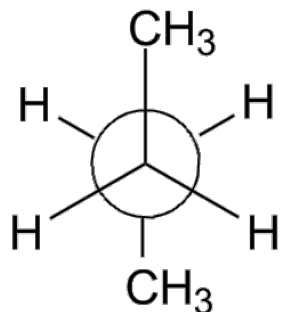
$$Z = \sum_i e^{-\beta E_i}$$

Conformational Enthalpy of Polymers

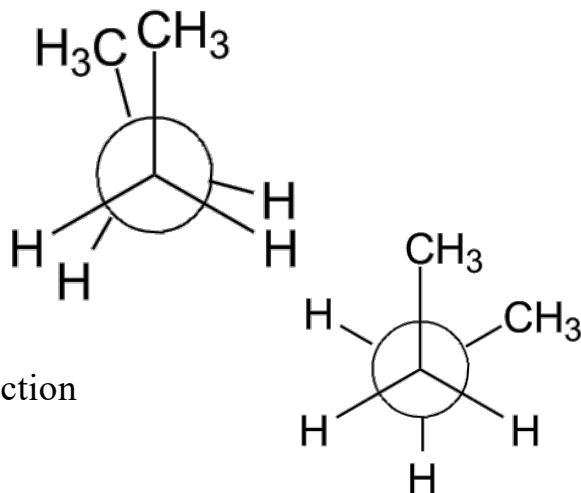
The Rotational Isomeric State Model of Volkenstein and Paul Flory (Nobel Prize)

Carbon has a tetrahedral bonding arrangement

For a chain of carbon, the two side groups interact with the side groups of neighboring carbons



For Butene



Neumann Projection

“Trans” is sterically the most favorable arrangement

“Gauche +” and “Gauche -” are less favorable

The Boltzmann equation gives the probability of a particular conformation, **Z is the partition function** or the sum of all the different Boltzmann expressions in an ensemble

$$P(\varphi_i) = \frac{\exp(-E(\varphi_i)/kT)}{Z}$$

$$Z = \sum_i e^{-\beta E_i}$$

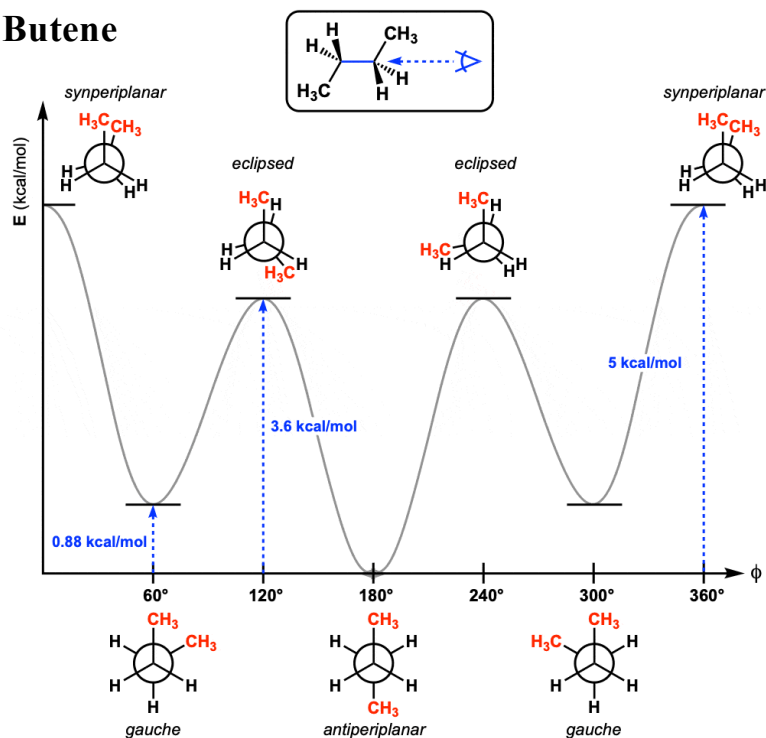
Conformational Enthalpy of Polymers

The Rotational Isomeric State Model of Volkenstein and Paul Flory (Nobel Prize)

Carbon has a tetrahedral bonding arrangement

For a chain of carbon the two side groups interact with the side groups of neighboring carbons

For Butene



“Trans” is sterically the most favorable arrangement

“Gauche +” and “Gauche -” are less favorable

The Boltzmann equation gives the probability of a particular conformation, **Z is the partition function** or the sum of all of the different Boltzmann expressions in an ensemble

$$P(\varphi_i) = \frac{\exp(-E(\varphi_i)/kT)}{Z}$$

$$Z = \sum_i e^{-\beta E_i}$$

Conformational Energy of Polymers

The Rotational Isomeric State Model of Volkenstein and Paul Flory (Nobel Prize)

Carbon has a tetrahedral bonding arrangement

For a chain of carbon, the two side groups interact with the side groups of neighboring carbons

For Butene

$$Z = 1 + \exp(-E_{g+}/kT) + \exp(-E_{g-}/kT) = 1 + 2\sigma$$

$$Z = \sum_i e^{-\beta E_i}$$

Helmholtz Free Energy and Entropy

$$F_P = -kT \cdot \ln Z ; \quad S_P = -\frac{\partial F_P}{\partial T}$$

$$P(\varphi_i) = \frac{\exp(-E(\varphi_i)/kT)}{Z}$$

Boltzmann equation where Z is number of states
(which depend on temperature and energy barriers)

Internal Energy

$$U = F_P + S_P T$$

-SUV
H A(F)
-pGT

Conformational Enthalpy of Polymers

The Rotational Isomeric State Model of Volkenstein and Paul Flory (Nobel Prize)

For a polymer with N carbons there are N-2 covalent bonds

The number of discrete conformation states per chain is n^{N-2} where n is the number of discrete rotational states for the chain, tttt, g⁻g⁻g⁻g⁻, g⁺g⁺g⁺g⁺, g⁺ttt, etc. for N = 4; N₁=1, N₄=4, etc. assuming no end effects

$$Z = \sum_{\{N_\eta\}} \frac{(N-2)!}{N_1! \dots N_v!} \exp(-N_1 E(\varphi_1)/kT) \dots \exp(-N_v E(\varphi_v)/kT)$$

Average rotational angle

$$\langle \cos \varphi \rangle = \frac{\sum_{i=1}^v \exp(-E(\varphi_i)/kT) \cos \varphi_i}{\sum_{i=1}^v \exp(-E(\varphi_i)/kT)} = \frac{1 - \sigma}{1 + 2\sigma}$$

Characteristic Ratio

$$C_\infty = \lim_{N \rightarrow \infty} \frac{\langle r^2 \rangle_0}{Nl^2} = \frac{(1 + \cos \theta) (1 + \langle \cos \varphi \rangle)}{(1 - \cos \theta) (1 - \langle \cos \varphi \rangle)}$$

θ is the bond angle

$$180^\circ - 109^\circ = 71^\circ$$

$$E_{g^\pm} = 2100 \text{ J/mole}$$

$$C_\infty = 3.6$$

Exp. 6.7

